

2013-056 \_\_\_\_\_ BWR Vessel & Internals Project (BWRVIP)

April 17, 2013

Document Control Desk  
U. S. Nuclear Regulatory Commission  
11555 Rockville Pike  
Rockville, MD 20852

Attention: Joseph Holonich

Subject: Project No. 704 – BWRVIP-271NP: BWR Vessel and Internals Project, Testing and Evaluation of the Browns Ferry Unit 2 120° Capsule”

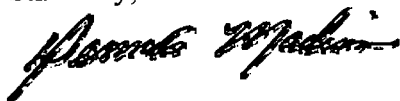
Enclosed are five (5) paper copies of the report “BWRVIP-271NP: BWR Vessel and Internals Project, Testing and Evaluation of the Browns Ferry Unit 2 120° Capsule,” EPRI Technical Report 3002000078, April 2013. This report is being transmitted to the NRC for information only.

This report describes testing and evaluation of the Browns Ferry Unit 2 120° capsule. These results will be used to monitor embrittlement as part of the BWRVIP ISP.

Please note that the enclosed report is non-proprietary and is available to the public by request to EPRI.

If you have any questions on this subject please call Ron DiSabatino (Exelon, BWRVIP Assessment Focus Group Chairman) at 610-765-5753.

Sincerely,



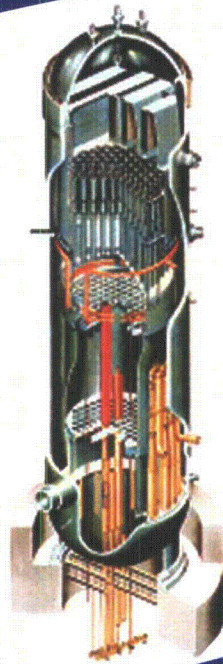
Dennis Madison  
Southern Nuclear  
Chairman, BWR Vessel and Internals Project

c: Gary Stevens, NRC

Together . . . Shaping the Future of Electricity

# BWRVIP-271NP: BWR Vessel and Internals Project

Testing and Evaluation of the Browns Ferry Unit 2 120° Capsule



# **BWRVIP-271NP: BWR Vessel and Internals Project**

Testing and Evaluation of the Browns Ferry Unit 2  
120° Capsule

**3002000078**

Final Report, April 2013

EPRI Project Manager  
R. Carter

Work to develop this product was completed under the EPRI Nuclear Quality Assurance Program  
in compliance with 10 CFR 50, Appendix B and 10 CFR 21,



## **DISCLAIMER OF WARRANTIES AND LIMITATION OF LIABILITIES**

THIS DOCUMENT WAS PREPARED BY THE ORGANIZATION(S) NAMED BELOW AS AN ACCOUNT OF WORK SPONSORED OR COSPONSORED BY THE ELECTRIC POWER RESEARCH INSTITUTE, INC. (EPRI). NEITHER EPRI, ANY MEMBER OF EPRI, ANY COSPONSOR, THE ORGANIZATION(S) BELOW, NOR ANY PERSON ACTING ON BEHALF OF ANY OF THEM:

(A) MAKES ANY WARRANTY OR REPRESENTATION WHATSOEVER, EXPRESS OR IMPLIED, (I) WITH RESPECT TO THE USE OF ANY INFORMATION, APPARATUS, METHOD, PROCESS, OR SIMILAR ITEM DISCLOSED IN THIS DOCUMENT, INCLUDING MERCHANTABILITY AND FITNESS FOR A PARTICULAR PURPOSE, OR (II) THAT SUCH USE DOES NOT INFRINGE ON OR INTERFERE WITH PRIVATELY OWNED RIGHTS, INCLUDING ANY PARTY'S INTELLECTUAL PROPERTY, OR (III) THAT THIS DOCUMENT IS SUITABLE TO ANY PARTICULAR USER'S CIRCUMSTANCE; OR

(B) ASSUMES RESPONSIBILITY FOR ANY DAMAGES OR OTHER LIABILITY WHATSOEVER (INCLUDING ANY CONSEQUENTIAL DAMAGES, EVEN IF EPRI OR ANY EPRI REPRESENTATIVE HAS BEEN ADVISED OF THE POSSIBILITY OF SUCH DAMAGES) RESULTING FROM YOUR SELECTION OR USE OF THIS DOCUMENT OR ANY INFORMATION, APPARATUS, METHOD, PROCESS, OR SIMILAR ITEM DISCLOSED IN THIS DOCUMENT.

REFERENCE HEREIN TO ANY SPECIFIC COMMERCIAL PRODUCT, PROCESS, OR SERVICE BY ITS TRADE NAME, TRADEMARK, MANUFACTURER, OR OTHERWISE, DOES NOT NECESSARILY CONSTITUTE OR IMPLY ITS ENDORSEMENT, RECOMMENDATION, OR FAVORING BY EPRI.

THE FOLLOWING ORGANIZATION PREPARED THIS REPORT:

**Electric Power Research Institute (EPRI)**

**MP Machinery & Testing, LLC**

**TransWare Enterprises Inc.**

THE TECHNICAL CONTENTS OF THIS DOCUMENT WERE PREPARED IN ACCORDANCE WITH THE EPRI NUCLEAR QUALITY ASSURANCE PROGRAM MANUAL THAT FULFILLS THE REQUIREMENTS OF 10 CFR 50 APPENDIX B, 10 CFR PART 21, ANSI N45.2-1977 AND/ OR THE INTENT OF ISO-9001 (1994). CERTIFICATION OF CONFORMANCE CAN BE OBTAINED FROM EPRI. BEFORE THE CONTENTS OF THIS DOCUMENT CAN BE APPLIED TO FULFILL QUALITY PROGRAM REQUIREMENTS, CONTRACTUAL ARRANGEMENTS BETWEEN THE USER AND EPRI MUST BE ESTABLISHED. USE OF THE CONTENTS OF THIS DOCUMENT IN NUCLEAR SAFETY OR NUCLEAR QUALITY APPLICATIONS MAY ALSO REQUIRE FURTHER ACCEPTANCE REVIEWS/ACTIONS PURSUANT TO USER'S INTERNAL PROCEDURES.

### **NOTE**

For further information about EPRI, call the EPRI Customer Assistance Center at 800.313.3774 or e-mail [askepri@epri.com](mailto:askepri@epri.com).

Electric Power Research Institute, EPRI, and TOGETHER...SHAPING THE FUTURE OF ELECTRICITY are registered service marks of the Electric Power Research Institute, Inc.

Copyright © 2013 Electric Power Research Institute, Inc. All rights reserved.

# ACKNOWLEDGMENTS

---

The following organizations prepared this report:

Electric Power Research Institute (EPRI)  
3420 Hillview Ave  
Palo Alto, CA 94304

Principal Investigators  
T. Hardin  
M. O'Connor

MP Machinery & Testing, LLC  
2161 Sandy Drive  
State College, PA 16803

Principal Investigator  
Dr. M. P. Manahan, Sr.

TransWare Enterprises Inc.  
1565 Mediterranean Drive  
Sycamore, IL 60178

Principal Investigator  
E. N. Jones

This report describes research sponsored by EPRI and its BWRVIP participating members.

---

This publication is a corporate document that should be cited in the literature in the following manner:

*BWRVIP-271NP: BWR Vessel and Internals Project, Testing and Evaluation of the Browns Ferry Unit 2 120° Capsule.* EPRI, Palo Alto, CA: 2013. 3002000078.



# PRODUCT DESCRIPTION

---

In the late 1990s, a Boiling Water Reactor Vessel and Internals Project (BWRVIP) Integrated Surveillance Program (ISP) was developed to improve the surveillance of the U.S. BWR fleet. This report describes testing and evaluation of the Browns Ferry Unit 2 120° capsule. These results will be used to monitor embrittlement as part of the BWRVIP ISP.

## Background

The BWRVIP ISP represents a major enhancement to the process of monitoring embrittlement for the U.S. fleet of BWRs. The ISP optimizes surveillance capsule tests while at the same time maximizing the quantity and quality of data, thus resulting in a more cost-effective program. The BWRVIP ISP provides more representative data that can be used to assess embrittlement in reactor pressure vessel beltline materials and improve trend curves in the BWR range of irradiation conditions.

## Challenges and Objectives

Neutron irradiation exposure reduces the toughness of reactor vessel steel plates, welds, and forgings. The objectives of this project were twofold:

- To document the results of neutron dosimetry and Charpy V-notch ductility tests for the surveillance materials (plate heat A0981-1 and weld heat BF2 ESW) in the Browns Ferry Unit 2 120° capsule
- To compare the results with the embrittlement trend prediction of the U.S. Nuclear Regulatory Commission (U.S. NRC) Regulatory Guide 1.99, Rev. 2

## Approach

The Browns Ferry Unit 2 120° capsule had been irradiated in the reactor since plant startup. The surveillance capsule contained flux wires for neutron flux monitoring, Charpy V-notch impact test specimens, and tensile specimens. The project team removed the capsule from the reactor in 2010 and transported it to facilities for testing and evaluation. The team used dosimetry to gather information about the neutron fluence accrual of specimens from the capsule. They then performed a neutron transport calculation in accordance with Regulatory Guide 1.190 and compared it to the results from the dosimetry. Testing of Charpy V-notch specimens was performed according to the American Society for Testing and Materials (ASTM) standards.

## Results and Findings

The report includes capsule neutron exposure and Charpy V-notch test results for Browns Ferry 2 surveillance plate heat A0981-1 and surveillance weld BF2 ESW (an electrosag weld of unknown heat number). The project compared irradiated Charpy data to unirradiated data in order to determine the shifts in Charpy index temperatures for the surveillance plate and weld materials due to irradiation. For the surveillance plate, results indicate a shift about 32% higher

than the prediction of Regulatory Guide 1.99, Revision 2, but within (predicted shift + margin). For the weld, the shift was about 2.3 times higher than the predicted shift and about 15% higher than (predicted shift + margin). Researchers also measured flux wires and determined fluence for the capsule.

### **Applications, Value, and Use**

Results of this work will be used in the BWRVIP ISP that integrates individual BWR surveillance programs into a single program. The ISP provides data of high quality to monitor BWR vessel embrittlement. The ISP results in significant cost savings to the BWR fleet and provides more accurate monitoring of embrittlement in BWR vessels.

### **Keywords**

BWR

Charpy testing

Mechanical properties

Radiation embrittlement

Reactor pressure vessel integrity

Reactor vessel surveillance program

# CONTENTS

---

<b>1 INTRODUCTION .....</b>	<b>1-1</b>
1.1 Implementation Requirements .....	1-1
<b>2 MATERIALS AND TEST SPECIMEN DESCRIPTION .....</b>	<b>2-1</b>
2.1 Dosimeters .....	2-1
2.2 Charpy V-Notch Specimens .....	2-1
2.2.1 Capsule Loading Inventory .....	2-1
2.2.2 Material Description and Properties .....	2-4
2.2.3 Chemical Composition .....	2-5
2.2.4 CVN Baseline Properties .....	2-5
2.3 Capsule Opening.....	2-12
<b>3 NEUTRON FLUENCE CALCULATION .....</b>	<b>3-1</b>
3.1 Description of the Reactor System .....	3-2
3.1.1 Reactor System Mechanical Design.....	3-2
3.1.2 Reactor System Material.....	3-4
3.1.3 Reactor Operating Data Inputs.....	3-5
3.1.3.1 Core Loading.....	3-6
3.1.3.2 Power History Data .....	3-6
3.1.3.3 Reactor State-Point Data.....	3-8
Beginning of Operation through Cycle 16 State Points.....	3-8
Projected Reactor Operation.....	3-8
Limitation of Fluence Projections.....	3-9
3.2 Calculation Methodology .....	3-10
3.2.1 Description of the RAMA Fluence Methodology .....	3-10
3.2.2 The RAMA Geometry Model for the Browns Ferry 2 Reactor.....	3-11
3.2.2.1 The Geometry Model.....	3-14
3.2.2.2 The Reactor Core and Core Reflector Models.....	3-15

3.2.2.3 The Core Shroud Model .....	3-16
3.2.2.4 The Downcomer Region Model .....	3-16
3.2.2.5 The Jet Pump Model .....	3-16
3.2.2.6 The Surveillance Capsule Model .....	3-16
3.2.2.7 The Reactor Pressure Vessel Model .....	3-17
3.2.2.8 The Vessel Insulation Model.....	3-17
3.2.2.9 The Inner and Outer Cavity Models .....	3-17
3.2.2.10 The Biological Shield Model .....	3-17
3.2.2.11 The Above-Core Component Models .....	3-17
The Top Guide Model .....	3-17
The Core Spray Sparger Model.....	3-18
3.2.2.12 The Below-Core Component Models .....	3-18
3.2.2.13 Summary of the Geometry Modeling Approach .....	3-18
3.2.3 RAMA Calculation Parameters.....	3-18
3.2.4 RAMA Neutron Source Calculation .....	3-19
3.2.5 RAMA Fission Spectra .....	3-19
3.3 Surveillance Capsule Activation and Fluence Results .....	3-19
3.3.1 Comparison of Predicted Activation to Plant-specific Measurements .....	3-20
3.3.1.1 Cycle 1 30° Flux Wire Holder Activation Analysis .....	3-20
3.3.1.2 Cycle 7 30° Surveillance Capsule Activation Analysis .....	3-21
3.3.1.3 Cycle 16 120° Surveillance Capsule Activation Analysis .....	3-21
3.3.1.4 Surveillance Capsule Activation Analysis Summary .....	3-22
3.3.2 Capsule Peak Fluence Calculations and Lead Factor Determinations .....	3-23
3.4 Capsule Fluence Uncertainty Analysis.....	3-23
3.4.1 Comparison Uncertainty.....	3-24
3.4.1.1 Operating Reactor Comparison Uncertainty .....	3-24
3.4.1.2 Benchmark Comparison Uncertainty .....	3-24
3.4.2 Analytic Uncertainty .....	3-24
3.4.3 Combined Uncertainty.....	3-25
<b>4 CHARPY TEST DATA .....</b>	<b>4-1</b>
4.1 Charpy Test Procedure.....	4-1
4.2 Charpy Test Data .....	4-2

---

<b>5 CHARPY TEST RESULTS .....</b>	<b>5-1</b>
5.1 Analysis of Impact Test Results.....	5-1
5.2 Irradiated Versus Unirradiated CVN Properties .....	5-1
<b>6 REFERENCES .....</b>	<b>6-1</b>
<b>A APPENDIX A – DOSIMETER ANALYSIS.....</b>	<b>A-1</b>
A.1 Dosimeter Material Description .....	A-1
A.2 Dosimeter Cleaning and Mass Measurement.....	A-1
A.3 Radiometric Analysis.....	A-4



# LIST OF FIGURES

---

Figure 2-1 Photograph of 120° capsule for Browns Ferry Unit 2 showing positive identification markings .....	2-3
Figure 2-2 Schematic drawing showing the locations of test specimens in the Browns Ferry Unit 2 120° surveillance capsule .....	2-4
Figure 2-3 Browns Ferry 2 plate A0981-1 (LT) unirradiated Charpy energy plot.....	2-8
Figure 2-4 Browns Ferry 2 weld BF2 ESW unirradiated Charpy energy plot .....	2-10
Figure 3-1 Planar view of Browns Ferry 2 at the core mid-plane elevation .....	3-3
Figure 3-2 Planar view of the Browns Ferry 2 RAMA quadrant model at the core mid-plane elevation .....	3-12
Figure 3-3 Axial view of the Browns Ferry 2 RAMA model .....	3-13
Figure 4-1 Illustration of digital optical comparator measurement of shear fracture area .....	4-2
Figure 5-1 Irradiated plate A0981-1 (Browns Ferry 2 120° capsule) Charpy energy plot .....	5-2
Figure 5-2 Irradiated plate A0981-1 (Browns Ferry 2 120° capsule) lateral expansion plot.....	5-3
Figure 5-3 Irradiated weld BF2 ESW (Browns Ferry 2 120° capsule) Charpy energy plot .....	5-4
Figure 5-4 Irradiated weld BF2 ESW (Browns Ferry 2 120° capsule) lateral expansion plot .....	5-5
Figure A-1 Packet G9 Cu dosimeter wire: prior to cleaning (left); and after cleaning/coiling (right).....	A-2
Figure A-2 Packet G9 Fe dosimeter wire: prior to cleaning (left); and after cleaning/coiling (right).....	A-2
Figure A-3 Packet G9 Ni dosimeter wire: prior to cleaning (left); and after cleaning/coiling (right).....	A-2
Figure A-4 Packet G10 Cu dosimeter wire: prior to cleaning (left); and after cleaning/coiling (right).....	A-3
Figure A-5 Packet G10 Fe dosimeter wire: prior to cleaning (left); and after cleaning/coiling (right).....	A-3
Figure A-6 Packet G10 Ni dosimeter Wire: prior to cleaning (left); and after cleaning/coiling (right).....	A-3



# LIST OF TABLES

Table 2-1 Browns Ferry 2 120° surveillance capsule specimen inventory .....	2-2
Table 2-2 Best estimate chemistry of Browns Ferry 2 surveillance plate A0981-1 .....	2-5
Table 2-3 Best estimate chemistry of Browns Ferry 2 surveillance weld BF2 ESW .....	2-5
Table 2-4 Unirradiated Charpy impact test data for surveillance plate A0981-1 (LT) .....	2-6
Table 2-5 Unirradiated Charpy impact test data for surveillance weld BF2 ESW .....	2-7
Table 2-6 Baseline CVN properties .....	2-7
Table 3-1 Summary of material compositions by region for Browns Ferry 2 .....	3-5
Table 3-2 Summary of the Browns Ferry 2 core loading inventory .....	3-7
Table 3-3 State-point data for each cycle in Browns Ferry 2 .....	3-9
Table 3-4 Comparison of specific activities for Browns Ferry 2 Cycle 1 30° flux wire holder wires (C/M) .....	3-20
Table 3-5 Comparison of specific activities for Browns Ferry 2 cycle 7 30° surveillance capsule flux wires (C/M) .....	3-21
Table 3-6 Comparison of specific activities for Browns Ferry 2 cycle 16 120° surveillance capsule flux wires (C/M) .....	3-22
Table 3-7 Comparison of activities for Browns Ferry 2 surveillance capsule flux wires .....	3-22
Table 3-8 Lead factors for Browns Ferry 2 30°, 120°, and 300° surveillance capsules .....	3-23
Table 3-9 Combined capsule fluence uncertainty for energy >1.0 MeV .....	3-25
Table 4-1 Irradiated Charpy V-Notch impact test results for base metal (heat A0981-1) specimens from the Browns Ferry 2 120° surveillance capsule .....	4-3
Table 4-2 Irradiated Charpy V-Notch impact test results for weld metal (heat BF2 ESW) specimens from the Browns Ferry 2 120° surveillance capsule .....	4-4
Table 4-3 Irradiated Charpy V-Notch impact test results for HAZ specimens from the Browns Ferry 2 120° surveillance capsule .....	4-4
Table 5-1 Effect of irradiation (E>1.0 MeV) on the notch toughness properties .....	5-6
Table 5-2 Comparison of actual versus predicted embrittlement .....	5-6
Table 5-3 Percent decrease in upper shelf energy .....	5-7
Table A-1 Wire dosimeter masses .....	A-4
Table A-2 GRSS specifications .....	A-5
Table A-3 Counting schedule for the dosimeter materials .....	A-6
Table A-4 Neutron-induced reactions of interest .....	A-6
Table A-5 Results of the radiometric analysis .....	A-6



# 1

## INTRODUCTION

---

Test coupons of reactor vessel ferritic beltline materials are irradiated in reactor surveillance capsules to facilitate evaluation of vessel fracture toughness in vessel integrity evaluations. The key values that characterize fracture toughness are the reference temperature of nil-ductility transition ( $RT_{NDT}$ ) and the upper shelf energy (USE). These are defined in 10CFR50 Appendix G [1] and in Appendix G of the ASME Boiler and Pressure Vessel Code, Section XI [2]. Appendix H of 10CFR50 [1] and ASTM E185-82 [3] establish the methods to be used for testing of surveillance capsule materials.

In the late 1990s the BWR Vessel and Internals Project (BWRVIP) initiated the BWRVIP Integrated Surveillance Program (ISP) [4], and the BWRVIP assumed responsibility for testing and evaluation of ISP capsules. The surveillance plate and weld from the Browns Ferry Nuclear Plant Unit 2 (hereinafter, Browns Ferry 2 or BF2) were designated as “ISP representative surveillance materials” to be tested by the ISP according to an approved capsule withdrawal and test schedule.

This report addresses the withdrawal and test of the Browns Ferry 2 120° capsule. The capsule was irradiated for 16 cycles of operation. The capsule was removed in February 2010 and testing and evaluation was completed in September 2012. The surveillance capsule contained flux wires for neutron flux monitoring, Charpy V-notch impact test specimens, and tensile specimens. The capsule was shipped to MP Machinery & Testing, LLC for opening and testing of the Charpy V-notch surveillance specimens. Evaluation of the fluence environment was conducted by TransWare Enterprises, Inc. Final evaluation of the Charpy test data and irradiated material properties and compilation of this report were performed by EPRI. The Charpy V-notch surveillance materials were tested per ASTM E185-82, and the information and the associated evaluations provided in this report have been performed in accordance with the requirements of 10CFR50 Appendix B [5].

This report compares the irradiated material properties of surveillance plate heat A0981-1 and surveillance weld BF2 ESW to their baseline (e.g., unirradiated) properties. The observed embrittlement (as characterized by  $\Delta T_{30}$ ) is compared to that predicted by U.S. Nuclear Regulatory Commission (U.S. NRC) Regulatory Guide 1.99, Rev. 2 [6]. Other BWRVIP ISP reports will integrate these shift results with the previous Browns Ferry 2 surveillance capsule results for a broader characterization of embrittlement behavior.

### 1.1 Implementation Requirements

The results documented in this report will be utilized by the BWRVIP ISP and by individual utilities to demonstrate compliance with 10CFR50, Appendix H, Reactor Vessel Material Surveillance Program Requirements. Therefore, the implementation requirements of 10CFR50, Appendix H govern and the implementation requirements of Nuclear Energy Institute (NEI) 03-08, Guideline for the Management of Materials Issues [7], are not applicable.

# 2

## MATERIALS AND TEST SPECIMEN DESCRIPTION

---

The General Electric (GE) designed Browns Ferry Unit 2 (BF2) 120° surveillance capsule was removed from the plant for analysis and testing during the February 2010 refueling outage. The capsule was a GE standard single basket design and contained a total of two Charpy packets and four tensile tubes. Within each Charpy packet were a total of 12 Charpy V-notch specimens and three high purity dosimetry wires. Each of the tensile tubes contained two tensile specimens. The 120° capsule is an original plant capsule, and has been irradiated in the plant since initial startup. This is the second surveillance capsule to be removed from BF2 and tested. The 30° capsule was removed during the Fall 1994 outage and was tested by GE [8].

### 2.1 Dosimeters

The dosimetry wires were located along the ends of the Charpy specimens during irradiation. Each of the two Charpy packets contained one high purity iron, copper, and nickel wire for fluence determination. Further details on the exact wire locations during the irradiation are provided in the capsule opening discussion given in Section 2.3. A detailed discussion of the radiometric analysis of the capsule dosimetry wires is provided in Appendix A.

### 2.2 Charpy V-Notch Specimens

The BF2 120° capsule Charpy V-notch and tensile specimen inventory, material descriptions, unirradiated (baseline) Charpy impact data, and previously measured capsule data are summarized in this section of the report.

#### 2.2.1 Capsule Loading Inventory

The BF2 120° surveillance capsule inventory is provided in Table 2-1. All of the capsule specimens, which include tensile specimens, Charpy specimens, and dosimeters, were recovered from the capsule basket. Testing was only performed on the 24 Charpy specimens, and the dosimetry wires were counted and weighed to determine specific activities. All eight of the tensile specimens (three base metal, three weld, and two HAZ) remain untested and are being held in reserve for future testing since there is no near-term use for tensile data. The technical advantage of storing the tensile specimens untested is that there will be options in the future for how these specimens will be used to obtain useful data. For example, the tensile specimen geometry is conducive to fabrication of subsized Charpy as well as miniaturized Charpy V-notch specimens. Further, research is currently underway to develop testing methods which will enable the determination of plane-strain fracture toughness data from Charpy-sized specimens. With these new technologies in view, there may be a need in the future for static and/or dynamic tensile data for use in the calculation of fracture toughness from experimental data obtained from Charpy specimens. Therefore, all of the tensile specimens have been placed into the archive storage so that they can be tested when necessary in the future. Similarly, the broken Charpy

specimen halves have been added to long-term archive storage for future use in miniature mechanical behavior specimen testing, chemistry analysis, and microstructural studies.

As indicated in Table 2-1, there were a total of two Charpy packets in the capsule, and each contained three dosimetry wires (one Fe wire, one Cu wire, and one Ni wire) and 12 Charpy specimens. Charpy packet G9 was found to contain all of the base metal test specimens as well as 4 weld specimens. Charpy packet G10 contained the remaining four weld specimens along with all of the HAZ specimens. The capsule and a schematic showing the position of the specimens within the capsule are shown in Figures 2-1 and 2-2, respectively.

**Table 2-1  
Browns Ferry 2 120° surveillance capsule specimen inventory**

Browns Ferry Unit 2 120° Surveillance Capsule Contents and Locations <sup>1</sup>							
Charpy Packet No. <sup>2</sup>	Number of Charpy Specimens			Number of Flux Wires			Relative Vertical Position
	Base	Weld	HAZ	Fe	Cu	Ni	
G9	8	4	0	1	1	1	Lowest in basket
G10	0	4	8	1	1	1	Highest in basket

<sup>1</sup> The capsule included tensile specimens, but the tensile specimens were not tested. Four tensile specimens for this capsule were located at the lowest axial position below Charpy packet G9 and four tensile specimens were located between Charpy packets G9 and G10.

<sup>2</sup> The packet numbers in this table are organized by axial position in the capsule with packet G9 at the lowest elevation in the reactor and packet G10 at the highest.

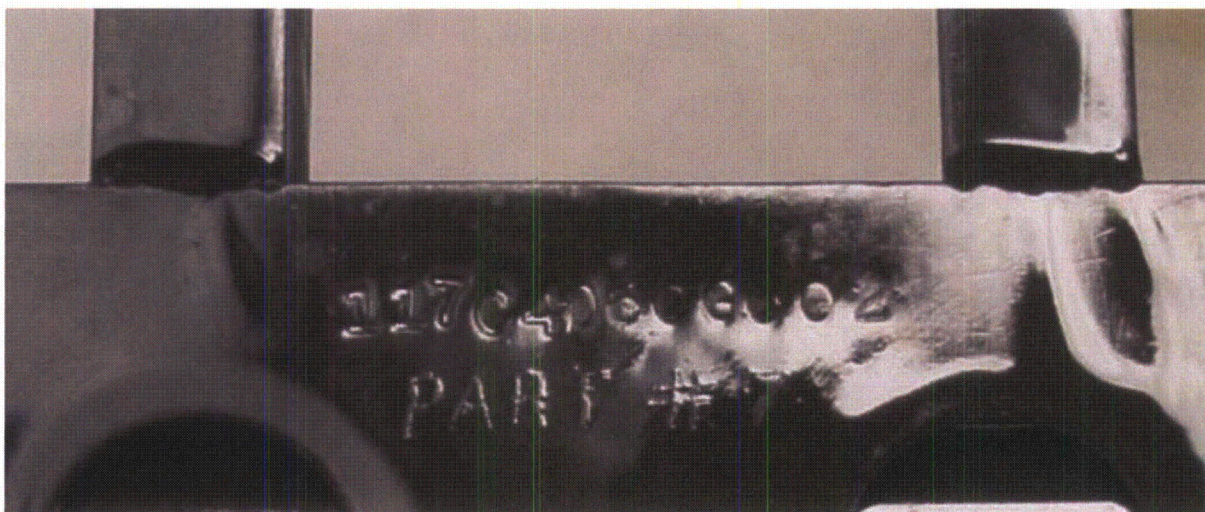


**Figure 2-1**  
**Photograph of 120° capsule for Browns Ferry Unit 2 showing positive identification markings**

Upper photograph shows the binary reactor code 26 in the upper left corner of the basket. The lower photograph shows the GE drawing number engraved on the basket outer surface. The Side which Faced the Pressure Vessel in the Plant is Facing Down in this Photograph.

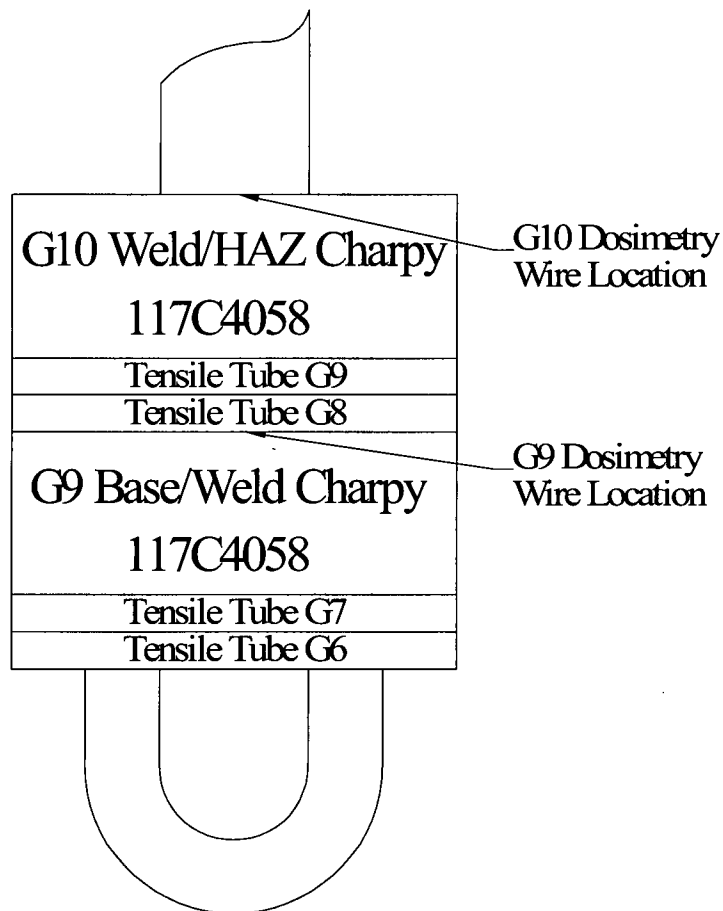


**Figure 2-2**  
Schematic drawing showing the locations of test specimens in the Browns Ferry Unit 2 120° surveillance capsule

### **2.2.2 Material Description and Properties**

The material descriptions, chemical compositions, and unirradiated (baseline) Charpy mechanical properties of the materials irradiated in the BF2 120° capsule are summarized below.

The BF2 surveillance base metal specimens were machined from plate heat number A0981-1 in the longitudinal orientation (LT). Unirradiated baseline data are available for the plate, weld and HAZ materials. All of the specimens were stamped on one end with the BF2 three-digit FAB codes assigned by GE.

The weld Charpy surveillance specimens were made by the electroslag-weld (ESW) process according to Babcock and Wilcox Weld Procedure WR-12-4 and subsequently heat treated to simulate the core region plate treatments [8]. The records regarding the identity of the weld wire heat number/flux lot combination used for the surveillance weld are not available [8,9]; therefore, the surveillance weld is referred to as BF2 ESW.

### 2.2.3 Chemical Composition

The best estimate chemical compositions of the surveillance plate A0981-1 and weld BF2 ESW are shown in Tables 2-2 and 2-3, respectively. Chemical compositions are presented in weight percent. If multiple measurements exist for a single specimen, those measurements are first averaged to yield a single value for that specimen, and then the different specimen averages are averaged to determine the best estimate for the surveillance heat.

**Table 2-2**  
Best estimate chemistry of Browns Ferry 2 surveillance plate A0981-1

Cu (wt%)	Ni (wt%)	P (wt%)	S (wt%)	Si (wt%)	Specimen ID	Source
0.14	0.55	0.007	0.011	0.19	N/A	Refs. 8 and 9
<b>0.14</b>	<b>0.55</b>	<b>0.007</b>	<b>0.011</b>	<b>0.19</b>	<b>← Best Estimate Average</b>	

**Table 2-3**  
Best estimate chemistry of Browns Ferry 2 surveillance weld BF2 ESW

Cu (wt%)	Ni (wt%)	P (wt%)	S (wt%)	Si (wt%)	Specimen ID	Source
0.20	0.33	0.010	0.011	0.09	N/A	Refs. 8 and 9
<b>0.20</b>	<b>0.33</b>	<b>0.010</b>	<b>0.011</b>	<b>0.09</b>	<b>← Best Estimate Average</b>	

### 2.2.4 CVN Baseline Properties

As noted above, the Browns Ferry 2 surveillance plate Charpy specimens are longitudinal (LT) specimens. Table 2-4 provides the unirradiated (baseline) Charpy test data for the A0981-1 surveillance plate material and Table 2-5 provides the unirradiated data for the weld [8].

The baseline test data were fit to a hyperbolic tangent curve using the computer program CVGRAPH [10]. Figures 2-3 and 2-4 show the fitted Charpy energy data curves for the unirradiated plate and weld, respectively. Table 2-6 summarizes the baseline (unirradiated) Charpy V-notch properties (index temperatures) of plate heat A0981-1 and weld heat BF2 ESW. In this table and throughout this report,  $T_{30}$  is the 30 ft-lb (41 J) transition temperature;  $T_{50}$  is the 50 ft-lb (68 J) transition temperature;  $T_{35\text{mil}}$  is the 35 mil (0.89 mm) lateral expansion temperature; and USE is the average energy absorption at full shear fracture appearance.

**Table 2-4**  
**Unirradiated Charpy impact test data for surveillance plate A0981-1 (LT)**

Specimen ID <sup>a</sup>	Temperature °F (C)	CVN ft-lb (J)	LE mils (mm)	Percent Shear (%)
E7B	-105.3 (-76.3)	4.33 (5.87)	5.0 (0.13)	3.7
E7J	-39.5 (-39.7)	21.92 (29.72)	15.0 (0.38)	11.7
E7C	6.3 (-14.3)	23.08 (31.29)	20.5 (0.52)	20.8
E63	40.1 (4.5)	73.68 (99.90)	54.0 (1.37)	38.2
E75	64.0 (17.8)	99.02 (134.25)	72.5 (1.84)	58.8
E74	97.2 (36.2)	107.05 (145.14)	70.5 (1.79)	60.3
E62	174.7 (79.3)	140.88 (191.01)	92.0 (2.34)	100.0
E5K	327.9 (164.4)	144.72 (196.21)	93.5 (2.37)	100.0

<sup>a</sup> All specimen IDs have a dot over the middle alphanumeric character.

**Table 2-5**  
**Unirradiated Charpy impact test data for surveillance weld BF2 ESW**

Specimen ID <sup>a</sup>	Temperature °F (C)	CVN ft-lb (J)	LE mils (mm)	Percent Shear (%)
EBJ	-49.7 (-45.4)	5.47 (7.42)	6.5 (0.17)	4.6
EAL	14.4 (-9.8)	28.06 (38.04)	21.5 (0.55)	12.7
EAE	50.0 (10.0)	47.89 (64.93)	40.0 (1.02)	22.5
EC3	81.3 (27.4)	22.40 (30.37)	25.0 (0.64)	28.3
EBU	119.1 (48.4)	83.90 (113.75)	63.5 (1.61)	50.3
EB6	204.3 (95.7)	102.15 (138.49)	79.0 (2.01)	79.3
EAK	301.6 (149.8)	113.53 (153.92)	88.0 (2.24)	100.0
EAD	373.8 (189.9)	110.62 (149.98)	84.5 (2.15)	100.0

<sup>a</sup> All specimen IDs have a dot over the middle alphanumeric character.

**Table 2-6**  
**Baseline CVN properties**

Material Identity	Material	T <sub>30</sub> °F (°C)	T <sub>50</sub> °F (°C)	T <sub>35mil</sub> °F (°C)	Upper Shelf Energy (USE) ft-lb (J)
A0981-1 (LT)	Browns Ferry 2 Surveillance Plate	-46.7 (-43.7)	-14.8 (-26.0)	-25.4 (-31.9)	137.8 (186.8)
BF2 ESW	Browns Ferry 2 Surveillance Weld	-52.5 (-46.9)	-19.5 (-28.6)	-29.5 (-34.2)	116.0 (157.3)

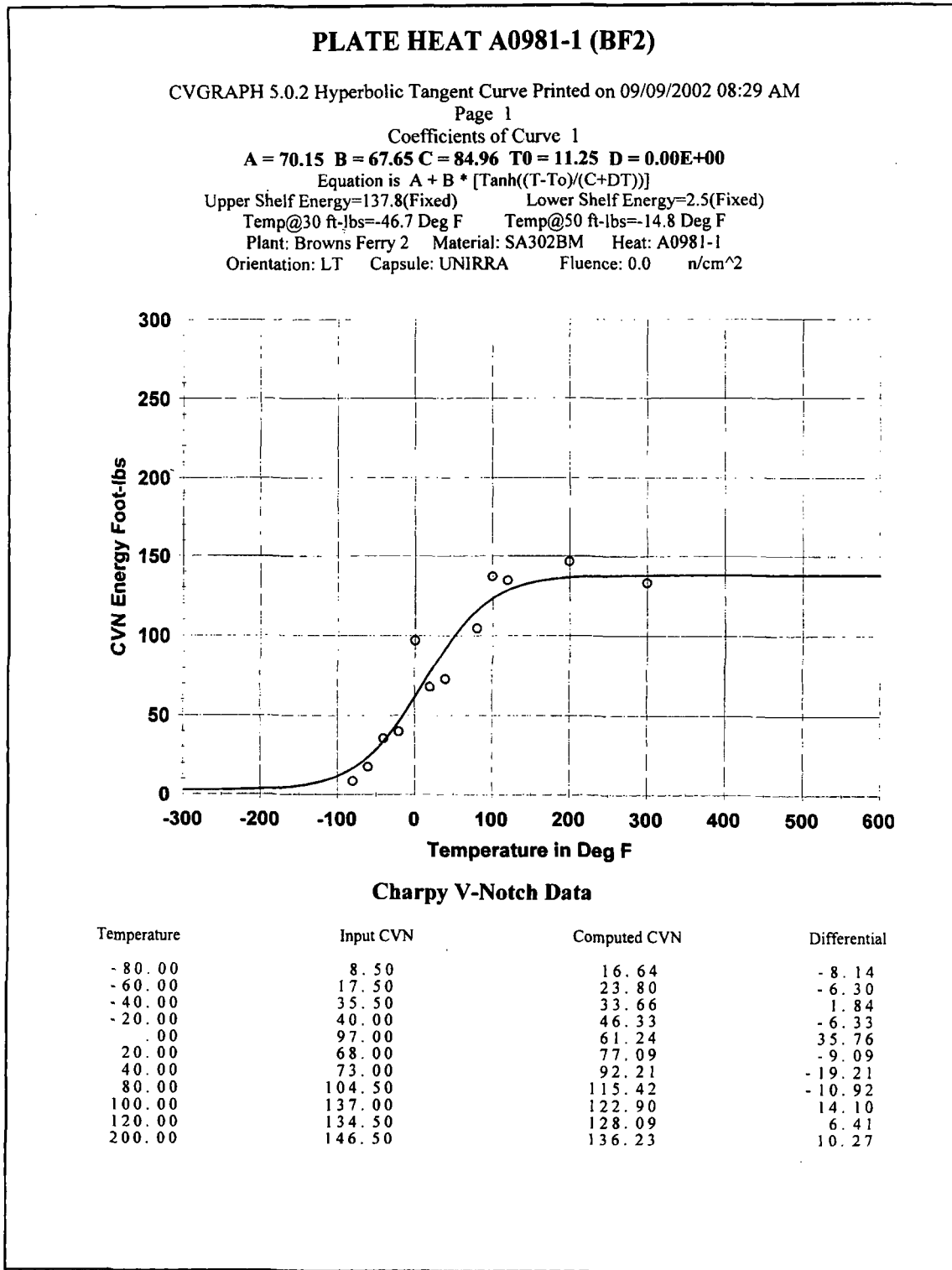


**Figure 2-3**  
**Browns Ferry 2 plate A0981-1 (LT) unirradiated Charpy energy plot**

**PLATE HEAT A0981-1 (BF2)**

Page 2

Plant: Browns Ferry 2 Material: SA302BM Heat: A0981-1  
Orientation: LT Capsule: UNIRRA Fluence: 0.0 n/cm<sup>2</sup>

**Charpy V-Notch Data**

Temperature	Input CVN	Computed CVN	Differential
300.00	133.00	137.65	- 4.65

Correlation Coefficient = .956

**Figure 2-3, continued**  
**Browns Ferry 2 plate A0981-1 (LT) unirradiated Charpy energy plot**

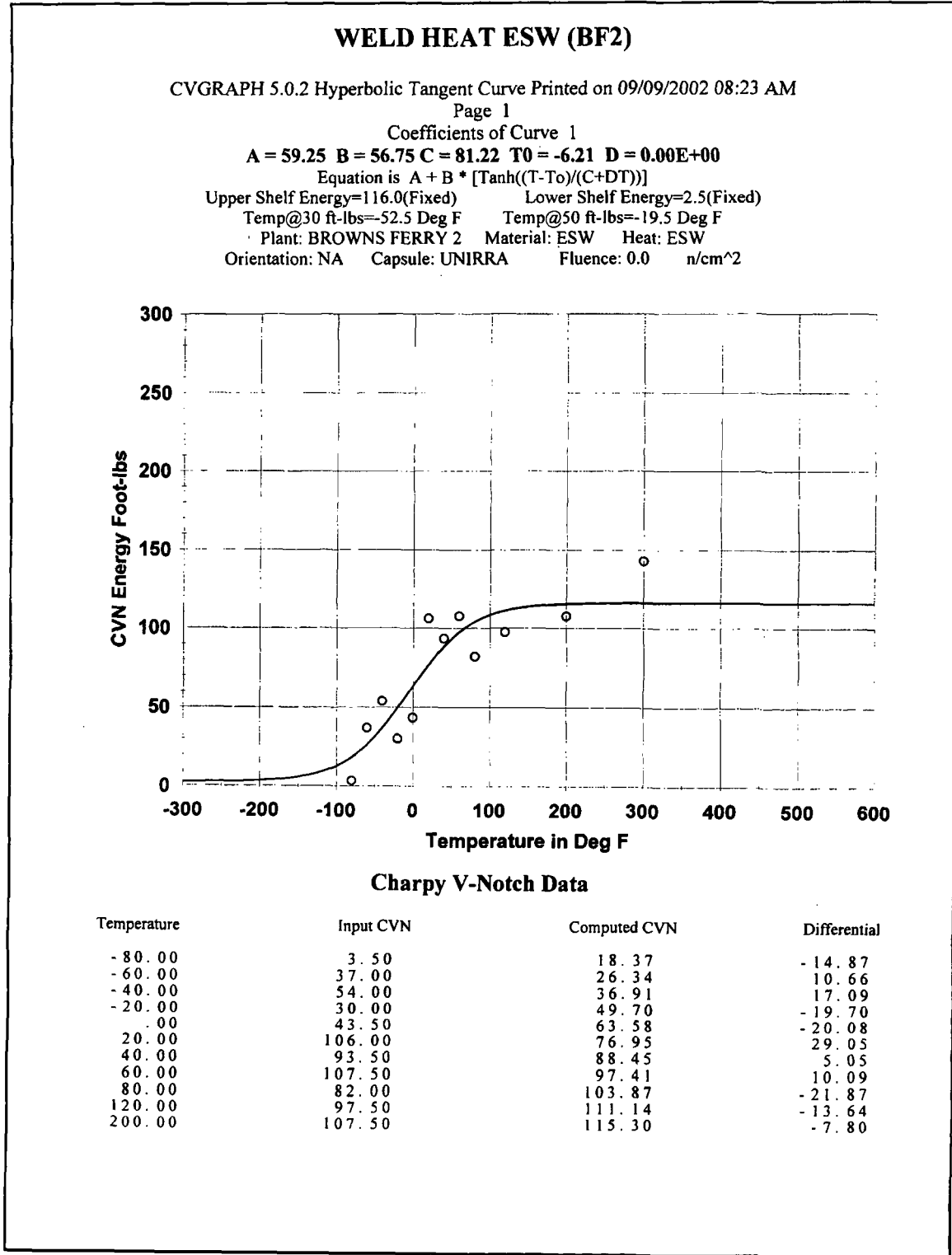


Figure 2-4  
 Browns Ferry 2 weld BF2 ESW unirradiated Charpy energy plot

**WELD HEAT ESW (BF2)**

Page 2

Plant: BROWNS FERRY 2    Material: ESW    Heat: ESW  
Orientation: NA    Capsule: UNIRRA    Fluence: 0.0    n/cm<sup>2</sup>

**Charpy V-Notch Data**

Temperature	Input CVN	Computed CVN	Differential
300.00	143.00	115.94	27.06

Correlation Coefficient = .891

Figure 2-4 (continued)  
Browns Ferry 2 weld BF2 ESW unirradiated Charpy energy plot

## **2.3 Capsule Opening**

The surveillance capsule was opened on April 11, 2012. As shown in Figure 2-1, the 120° capsule consisted of a single basket attached to the lead tube. The outside of the capsule had identification markings which could be clearly read. The capsule was marked with the correct binary reactor code number 26, which agrees with the markings reported on GE Drawing 129B3578 entitled, "Surveillance Program Number Identification of GE Reactors." The capsule basket was also engraved with drawing number 117C4060B007, Part Number 7, and this marking is consistent with the markings observed on the 30° capsule basket described in [8]. As indicated in Figure 2-2, the capsule basket contained two Charpy packets and four tensile tubes.

Referring to Figure 2-1, the lead tube is positioned on the top surface of the basket in the photograph. Therefore, the surface that is facing down in the photograph was facing the vessel during irradiation. The hook at the top of the photograph is the vessel lower attachment hook, and it was on the bottom of the capsule when the capsule was installed in the plant. The Charpy packet end tabs are on the right side in Figure 2-1. Moving up from the bottom of the capsule, the first item in the capsule was tensile tube G6, then tensile tube G7, followed by Charpy packet G9. Above Charpy packet G9, the remaining two tensile tubes G8 and G9 were loaded with Charpy packet G10 at the highest elevation in the plant.

Attention was paid to the location of the Charpy specimens and the dosimetry wire locations during disassembly of the Charpy packets. Each packet was found to contain one Fe, one Cu, and one Ni dosimetry wire along the ends of the Charpy specimens at the locations shown in Figure 2-2. The wire locations along the ends of the Charpy specimens were on the top side of the Charpy packets when the capsule was in the plant. Therefore, the wires were irradiated in a horizontal position in the reactor. The identifications assigned to the dosimetry wires indicate the Charpy packet from which they were recovered. The wires and Charpy specimens were placed in individually marked containers for positive identification throughout the work.

# 3

## NEUTRON FLUENCE CALCULATION

---

The Browns Ferry 2 120° capsule was irradiated for 16 cycles of operation. The surveillance capsule was placed in the reactor's 120° capsule holder prior to cycle 1 and was removed following cycle 16 for a total irradiation period of 22.9 effective full power years (EFPY). The surveillance capsule included copper, iron, and nickel flux wire dosimetry specimens.

Evaluation of the surveillance capsule specimens requires knowledge of the neutron irradiation environment. The neutron flux density, neutron energy spectrum, and neutron fluence are required at the surveillance capsule location. The NRC has established guidelines in Regulatory Guide 1.190 [11] for determining best estimate values of flux, energy spectrum, and fluence for RPV damage assessments using particle transport methods. These guidelines are not specifically intended for use in surveillance capsule evaluations; however, they do provide a suitable framework to support the development of accurate neutron transport analysis models for surveillance capsule evaluations.

This report documents the application of the modeling and analysis guidelines provided in [11] to determine the surveillance capsule accumulated irradiation and capsule specimen neutron fluence of the Browns Ferry 2 120° ISP capsule flux wires. Additionally, the accumulated irradiation for the 30° capsule, removed at the end of cycle 7, and the 30° flux wires, removed at the end of cycle 1, were determined. The neutron fluence was also calculated for the 300° capsule at the projected time of removal, and for the 120° capsule at the end of cycle 16 and at the end of the reactor's extended design life of 54 EFPY. The fluence and activation values presented in this report were calculated using the RAMA Fluence Methodology [12] (hereinafter referred to as "RAMA"). The specific activities predicted by RAMA are compared to the activity measurements reported in Appendix A.

RAMA was developed for the Electric Power Research Institute, Inc. (EPRI) and the Boiling Water Reactor Vessel and Internals Project (BWRVIP) for the purpose of calculating neutron fluence in Boiling Water Reactor (BWR) components. As prescribed in Regulatory Guide 1.190, RAMA has been benchmarked against industry standard benchmarks for both pressurized water reactor (PWR) and BWR designs. In addition, RAMA has been compared with several plant-specific dosimetry measurements and reported fluence from several commercial operating reactors. The results of the benchmarks and comparisons to measurements show that RAMA accurately predicts specimen activities, RPV fluence, and vessel internal component fluence in all light water reactor types. Under funding from EPRI and the BWRVIP, the RAMA methodology has been reviewed by the U.S. NRC and subsequently given generic approval for determining fast neutron fluence in BWR pressure vessels [13] and vessel internal components that include the core shroud and top guide [14].

### 3.1 Description of the Reactor System

This section provides an overview of the reactor design and operating data inputs that were used to develop the Browns Ferry 2 reactor fluence model. All reactor design and operating data inputs used to develop the model were plant-specific and were provided by Tennessee Valley Authority (TVA). The inputs for the fluence geometry model were developed from design and as-built drawings for the reactor pressure vessel, vessel internals, fuel assemblies, and containment regions. The reactor operating data inputs were developed from core simulator data that provided a historical accounting of how the reactor operated for cycles 9 through 16. Core simulator data was not available for cycles 1 through 8. Data for these cycles was approximated using information from the following sources: 1) cycle summary reports, 2) spreadsheet data, and 3) cycle 9 data for axial power shapes, water densities, and fuel assembly orientation. Projections for cycle 17 to the end of the reactor's extended operating life were based on the reactor's operating history for cycle 16.

#### 3.1.1 Reactor System Mechanical Design

Browns Ferry 2 is a General Electric BWR/4 class reactor with a core loading of 764 fuel assemblies. Browns Ferry 2 began commercial operation in 1975 with a design rated power of 3293 MWt. At the beginning of cycle 11 the rated power was increased to 3458 MWt. At the time of this fluence analysis, Browns Ferry 2 had completed 16 cycles of operation.

Figure 3-1 illustrates the basic planar configuration of the Browns Ferry 2 reactor at an axial elevation near the reactor core mid-plane. All of the radial regions of the reactor that are required for fluence projections are shown. Beginning at the center of the reactor and projecting outward, the regions include: the core region, including control rod locations and fuel assembly locations (fuel locations are shown only for the 0 to 90 degree quadrant); core reflector region (bypass water); central shroud wall; downcomer water region including the jet pumps; reactor pressure vessel (RPV) wall; cavity between RPV and insulation; insulation; cavity region between the insulation and biological shield; and biological shield (concrete wall).

The mechanical design inputs that were used to construct the Browns Ferry 2 fluence geometry model included as-built and nominal design dimensional data. As-built data for the reactor components and regions of the reactor system is always preferred when constructing plant-specific models; however, as-built data is not always available. In these situations, nominal design information is used.

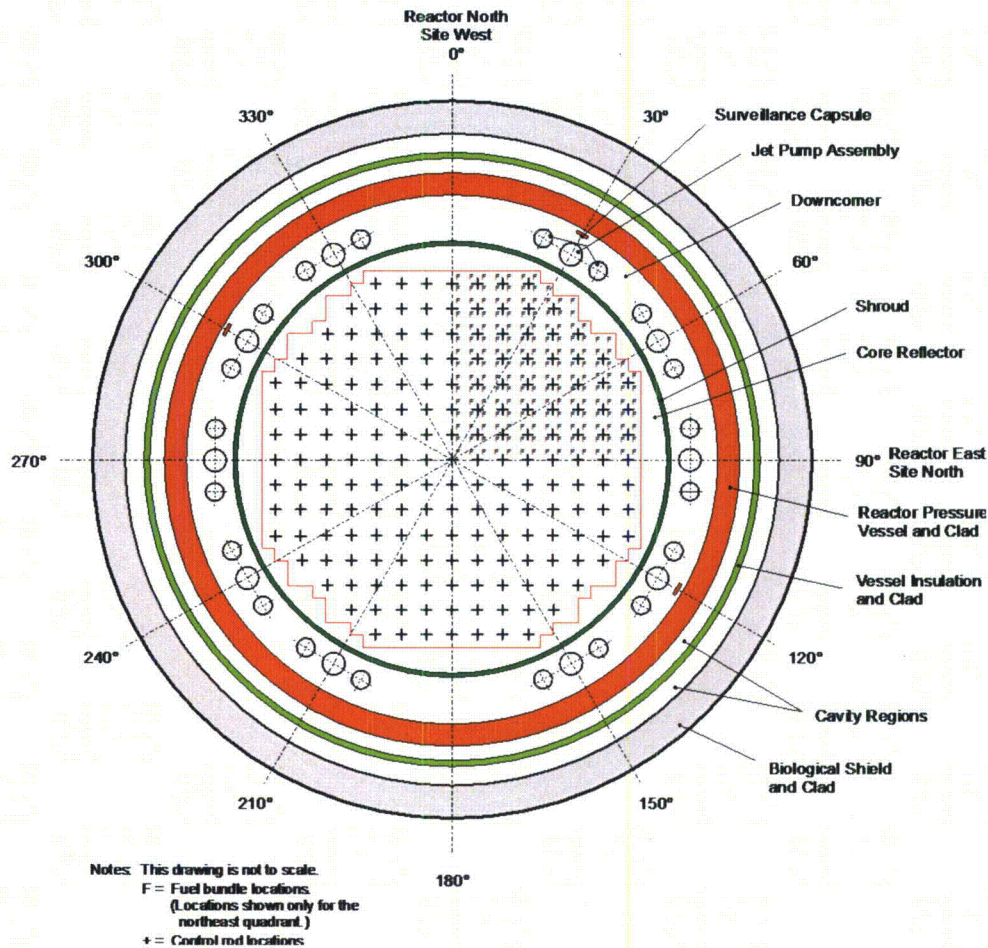


**Figure 3-1**  
Planar view of Browns Ferry 2 at the core mid-plane elevation

For the Browns Ferry 2 fluence model, the predominant dimensional information used to construct the fluence model was nominal design data. As-built data was available for the following dimensions:

- Jet pump mixer pipe radial location
- Reactor pressure vessel cladding inner radius

Another important component of the fluence analysis is the accurate description of the surveillance capsules in the reactor. It is shown in Figure 3-1 that three surveillance capsules were initially installed in the Browns Ferry 2 reactor. The capsules were attached radially to the inside surface of the RPV (looking outward from the core region) at the 30°, 120°, and 300° azimuths. Surveillance capsules are used to monitor the radiation accumulated in the reactor over a period of time. The importance of surveillance capsules in fluence analyses is that they contain flux wires that are irradiated during reactor operation. When a capsule is removed from the reactor, the irradiated flux wires are evaluated to obtain activity measurements. These measurements are used to validate the fluence model. Three sets of flux wires have been removed from the Browns Ferry 2 reactor and analyzed. (See Section 3.4, which presents a comparison of the calculated-to-measured capsule results.)

### **3.1.2 Reactor System Material**

Each region of the reactor is comprised of materials that include reactor fuel, steel, water, insulation, concrete, and air. Accurate material information is essential for the fluence evaluation as the material compositions determine the scattering and absorption of neutrons throughout the reactor system and, thus, affect the determination of neutron fluence in the reactor components.

Table 3-1 provides a summary of the materials for the various components and regions of the Browns Ferry 2 reactor. The material attributes for the steel, insulation, concrete, and air compositions (i.e. material densities and isotopic concentrations) are assumed to remain constant for the operating life of the reactor. The attributes of the fuel compositions in the reactor core region change continuously during an operating cycle due to changes in power level, fuel burnup, control rod movements, and changing moderator density levels (voids). Because of the dynamics of the fuel attributes with reactor operation, several state-point data sets are used to describe the operating states of the reactor for each operating cycle. The number of data sets used in this analysis is presented in Section 3.1.3.3.

**Table 3-1**  
**Summary of material compositions by region for Browns Ferry 2**

Region	Material Composition
Control Rods and Guide Tubes	Stainless Steel, B <sub>4</sub> C
Core Support Plate	Stainless Steel
Fuel Support Piece	Stainless Steel
Fuel Assembly Lower Tie Plate	Stainless Steel, Zircaloy, Inconel
Reactor Core	<sup>235</sup> U, <sup>238</sup> U, <sup>239</sup> Pu, <sup>240</sup> Pu, <sup>241</sup> Pu, <sup>242</sup> Pu, O <sub>fuel</sub> , Zircaloy
Reactor Coolant / Moderator	Water
Core Reflector	Water
Fuel Assembly Upper Tie Plate	Stainless Steel, Zircaloy, Inconel
Top Guide	Stainless Steel
Core Spray Sparger Pipes	Stainless Steel
Core Spray Sparger Flow Areas	Water
Shroud	Stainless Steel
Downcomer Region	Water
Jet Pump Riser and Mixer Flow Areas	Water
Jet Pump Riser and Mixer Metal	Stainless Steel
Jet Pump Riser Brace and Pads	Stainless Steel
Surveillance Capsule Specimens	Carbon Steel
Reactor Pressure Vessel Clad	Stainless Steel
Reactor Pressure Vessel Wall	Carbon Steel
Cavity Regions	Air (Nitrogen)
Insulation Clad	Stainless Steel
Insulation	Aluminum Foil
Biological Shield Clad	Carbon Steel
Biological Shield Wall	Reinforced Concrete

### 3.1.3 Reactor Operating Data Inputs

An accurate evaluation of reactor vessel and component fluence requires an accurate accounting of the reactor's operating history. The primary reactor operating parameters that affect the determination of fast neutron fluence in light water reactors include reactor power levels, core power distributions, coolant water density distributions, and fuel material (isotopic) distributions.

### 3.1.3.1 Core Loading

It is common in BWRs that more than one fuel assembly design may be loaded in the reactor core in any given operating cycle. For fluence evaluations, it is important to account for the fuel assembly designs that are loaded in the core in order to accurately represent the neutron source distribution at the core boundaries (i.e. peripheral fuel locations and the top and bottom fuel elevations).

Eleven different fuel assembly designs were loaded in the Browns Ferry 2 reactor during the period included in this evaluation. Table 3-2 provides a summary of the fuel designs loaded in the reactor core for each evaluated operating cycle. The cycle core loading provided by TVA was used to identify the fuel assembly designs in each cycle and their location in the core loading inventory. (Note that fuel loadings for cycle 12 were divided into three individual periods, identified as 12A, 12B and 12C.) For each cycle, appropriate fuel assembly models were used to build the reactor core region of the Browns Ferry 2 RAMA fluence model.

### 3.1.3.2 Power History Data

Reactor power history is the measure of reactor power levels and core exposure on a continual or periodic basis. For this fluence evaluation, the power history for the Browns Ferry 2 reactor was developed from power history inputs provided by TVA. The power history data showed that Browns Ferry 2 started commercial operation with a design rated thermal power of 3293 MWt for cycles 1 through 10 and implemented a measurement uncertainty recovery (MUR) power uprate of 3458 MWt at the beginning of cycle 11. It was assumed in this analysis that all future cycles would operate at the 3458 MWt power level.

The power history data for Browns Ferry 2 included daily power levels for most cycles. When daily power histories were not available, average power levels were constructed based on exposure accumulation using the core simulator codes. This data was used to calculate the capsule and vessel fluences. Periods of reactor shutdown due to refueling outages and other events were also accounted for in the model. The power history data was verified by comparing the calculated energy production in effective full power years with power production records provided by TVA. Table 3-3 lists the accumulated EFPY at the end of each cycle for this fluence evaluation.

**Table 3-2**  
**Summary of the Browns Ferry 2 core loading inventory**

Cycle	7x7 Designs	8x8 Designs						9x9 Designs		10x10 Designs		Dominant Peripheral Design
	GE3	GE4	GE5	GE6	GE7	QUAD+ <sup>1</sup>	GE9	GE11	GE13	GE14	ATR-10	
1	764											GE3
2	632	132										GE3
3	364	168	232									GE3
4	124	168	232	240								GE3
5		123	153	488								GE4
6			70	354	336	4						GE7
7				212	388	4	160					GE7
8				4	580	4	176					GE7
9					348		216	200				GE7
10					148		200	200	216			GE9
11							48	200	516			GE11
12A									764			GE13
12B									764			GE13
12C								49	715			GE13
13								111	281	372		GE11
14									149	335	280	GE13
15										111	653	GE14
16+ <sup>2</sup>											764	ATRIUM-10

<sup>1</sup> Due to lack of detailed information on QUAD+ design, these lead test assemblies (LTAs) were modeled as GE6 bundles.

<sup>2</sup> Cycles 17 and beyond use cycle 16 data for projecting fluence to the end of the extended plant license period.

### 3.1.3.3 Reactor State-Point Data

Cycles 1 through 8 of Browns Ferry 2 were derived from Cycle Summary Reports and plant data spreadsheets, which contained bundle average exposures. Radial power shapes were calculated based on this bundle average exposure data. Data from cycle 9 was used to provide axial power shapes, water densities, and fuel assembly orientation for cycles 1 through 8. This represented the best available information for these cycles.

Core simulator data was provided by TVA to characterize the historical operating conditions of Browns Ferry 2 for cycles 9 through 16 and cycle projections. The data calculated with core simulator codes represents the best-available information about the reactor core's operating history over the reactor's operating life. In this analysis, the core simulator data provided by TVA was processed by TransWare to generate state-point data files for input to the RAMA fluence model. The state-point files included three-dimensional data arrays that described core power distributions, fuel exposure distributions, fuel materials (isotopics), and coolant water densities.

A separate neutron transport calculation was performed for each of the state points tallied in Table 3-3. The calculated neutron flux for each state point was combined with the appropriate power history data described above in order to provide an accurate accounting of the fast neutron fluence for the reactor pressure vessel. Fluence projections to the end of the reactor's design life and extended design life were performed using projected equilibrium cycles. Equilibrium cycles are discussed below.

#### Beginning of Operation through Cycle 16 State Points

A total of 170 state points were used to represent the operating history for the first 16 operating cycles of Browns Ferry 2. These state points were selected from hundreds of exposure points that were calculated with the core simulator code. The hundreds of exposure points were evaluated and grouped into a fewer number of exposure ranges in order to reduce the number of transport calculations required to perform the fluence evaluation. Several criteria were used in the determination of the exposure ranges, including evaluations of core thermal powers, core flows, core power profiles, and control rod patterns. In determining exposure ranges, it is assumed that there will be at least one exposure step in that range that would accurately represent the average operating conditions of the reactor over that range. This single exposure step is then referred to as the "state point". Table 3-3 shows the number of state points used for each cycle in this fluence evaluation.

#### Projected Reactor Operation

Projections of plant operations beyond cycle 16 are represented with an "equilibrium" cycle that incorporates the best-available information on expected cycle length, fuel bundle loading, and operating strategies for future cycles. Cycle 16, at a thermal power level of 3458 MWt, is used as the equilibrium cycle for this analysis to project fluence to the end of the extended plant design life of 54 EFPY.

**Table 3-3**  
**State-point data for each cycle in Browns Ferry 2**

Cycle Number	Number of State Points	Rated Thermal Power <sup>1</sup> (MWt)	Accumulated Effective Full Power Years (EFPY)
1	3	3293	1.3
2	3	3293	2.0
3	3	3293	3.0
4	3	3293	4.4
5	3	3293	5.5
6	3	3293	6.8
7	3	3293	8.1
8	3	3293	9.4
9	20	3293	10.7
10	17	3293	12.2
11	19	3458	14.0
12	17	3458	15.7
13	21	3458	17.6
14	19	3458	19.4
15	17	3458	21.3
16	16	3458	22.9
17+ <sup>2</sup>	16	3458	54.0

<sup>1</sup>The rated thermal power is listed for each cycle. The actual power levels were used for the individual state-point calculations for cycles 1-16.

<sup>2</sup>Cycles 17 and beyond use cycle 16 data for projecting fluence to the end of the extended plant license.

### Limitation of Fluence Projections

Some of the fluence values presented in this report are based on projections of the operation of Browns Ferry 2 beyond the current operating cycle. Projections are performed using an assumed equilibrium cycle. The significance of the equilibrium cycle is that it defines the flux profiles that are used to project fluence into the future. Providing that the design basis for the equilibrium cycle does not change appreciably, projections based on the equilibrium cycle should remain bounding through 54 EFPY to support licensing, in-service inspection, and flaw evaluation activities.

If the design basis for the equilibrium cycle changes at any point in time that would result in a significant change to the flux profiles for the equilibrium cycle, then a new evaluation is needed. Operating conditions, if changed, that could impact the validity of the equilibrium cycle include power uprates, introduction of new fuel designs, changes in projected cycle lengths, changes in core loading strategies, changes in reactor flow, or other changes that could alter the flux profiles used in the fluence projections.

## **3.2 Calculation Methodology**

The Browns Ferry 2 capsule evaluation was performed using the RAMA Fluence Methodology software package [12]. RAMA and the application of RAMA to the Browns Ferry 2 reactor are described in this section.

### **3.2.1 Description of the RAMA Fluence Methodology**

The RAMA Fluence Methodology (RAMA) is a system of computer codes, a data library, and an uncertainty methodology that determines best-estimate fluence in light water reactor pressure vessels and vessel components. The primary codes that comprise the RAMA methodology include model builder codes, a particle transport code, and a fluence calculator code. The data library contains nuclear cross sections and response functions that are needed for each of the codes. The uncertainty methodology is used to determine the uncertainty and bias in the best-estimate fluence calculated by the software.

The primary inputs for RAMA are mechanical design parameters and reactor operating history data. The mechanical design inputs are obtained from plant-specific design drawings, which include as-built measurements when available. The reactor operating history data is obtained from reactor core simulator codes, system heat balance calculations, daily operating logs, and cycle summary reports that describe the operating conditions of the reactor over its operating lifetime. The primary outputs from RAMA calculations are neutron flux, neutron fluence, dosimetry activation, and an uncertainty evaluation.

The model builder codes consist of geometry and material processor codes that generate input for the particle transport code. The geometry model builder code uses mechanical design inputs and meshing specifications to generate three-dimensional geometry models of the reactor. The material processor code uses reactor operating data inputs to process fuel materials, structural materials, and water densities that are consistent with the geometry meshing generated by the geometry model builder code.

The particle transport code performs three-dimensional neutron flux calculations using a deterministic, multigroup, particle transport theory method with anisotropic scattering. The primary inputs prepared by the user for the transport code include the geometry and material data generated by the model builder codes and numerical integration and convergence parameters for the iterative transport calculation. The transport solver is coupled with a general geometry modeling capability based on combinatorial geometry techniques. The coupling of general geometry with a deterministic transport solver provides a flexible, accurate, and efficient tool for calculating neutron flux in light water reactor pressure vessels and vessel components. The primary output from the transport code is the neutron flux in multigroup form.

The fluence calculator code determines fluence and activation in the reactor pressure vessel and vessel components over specified periods of reactor operation. The primary inputs to the fluence calculator include the multigroup neutron flux from the transport code, response functions for the various materials in the reactor, reactor power levels for the operating periods of interest, the specification of which components to evaluate, and the energy ranges of interest for evaluating neutron fluence. The fluence calculator includes treatments for isotopic production and decay that are required to calculate specific activities for irradiated materials. The reactor operating history is generally represented with several reactor state points that represent the various power levels and core power shapes generated by the reactor over the life of the plant. These detailed state points are combined with the daily reactor power levels to produce accurate estimates of the fluence and activations accumulated in the plant.

The uncertainty methodology provides an assessment of the overall accuracy of the RAMA Fluence Methodology. Variances in the dimensional data, reactor operating data, dosimetry measurement data, and nuclear data are evaluated to determine if there is a statistically significant bias in the calculated results that might affect the determination of the best-estimate fluence for the reactor. The plant-specific results are also weighted with comparative results from experimental benchmarks and other plant analyses and analytical uncertainties pertaining to the methodology to determine if the plant-specific model under evaluation is statistically acceptable as defined in Regulatory Guide 1.190.

The RAMA nuclear data library contains atomic mass data, nuclear cross-section data, and response functions that are needed in the material processing, transport, fluence, and reaction rate calculations. The cross-section data and response functions are based on the BUGLE-96 nuclear data library [15] and the VITAMIN-B6 data library [16].

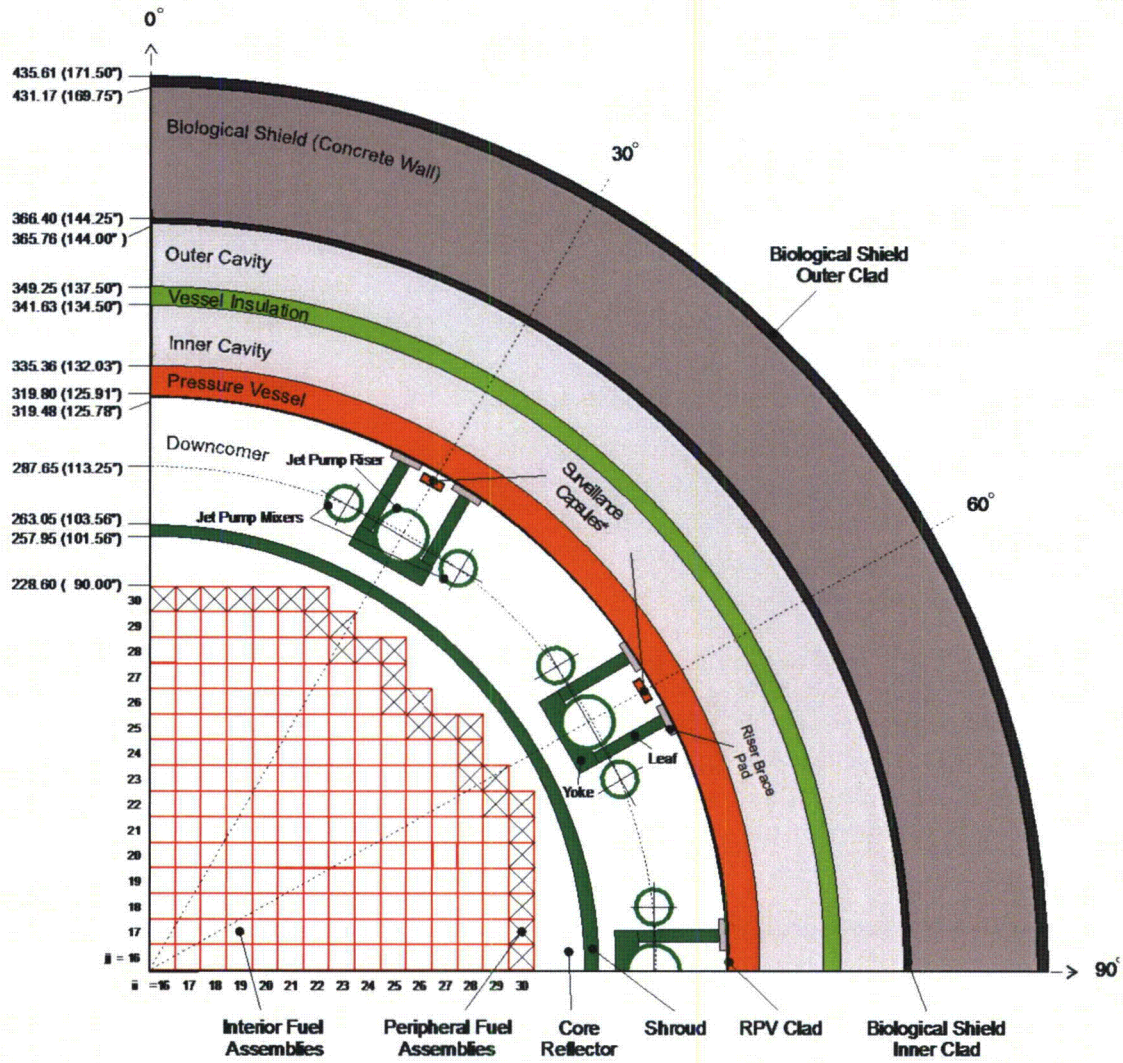
The RAMA Fluence Methodology is described in the Theory Manual [17]. The general procedures for using the methodology are presented in the Procedures Manual [18].

### **3.2.2 The RAMA Geometry Model for the Browns Ferry 2 Reactor**

Section 3.1 described the design inputs that were provided by TVA for the Browns Ferry 2 reactor fluence evaluation. These design inputs were used to develop a plant-specific, three-dimensional computer model of the Browns Ferry 2 reactor with the RAMA Fluence Methodology.

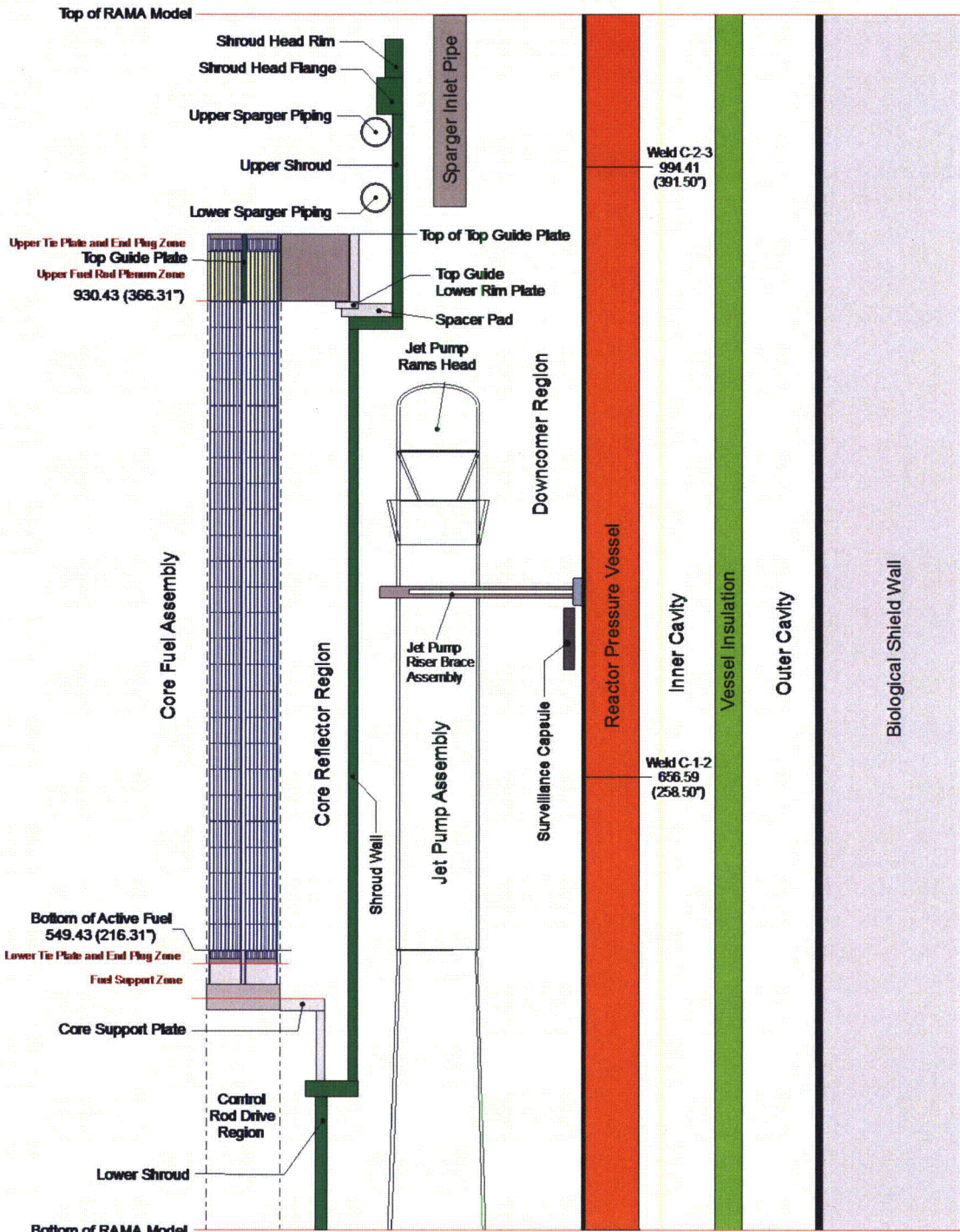
Figures 3-2 and 3-3 provide general illustrations of the primary components, structures and regions developed for the Browns Ferry 2 fluence model. Figure 3-2 shows the planar configuration of the reactor model at an elevation corresponding to the reactor core mid-plane elevation. Figure 3-3 shows an axial configuration of the reactor model. Note that the figures are not drawn to scale. They are intended only to provide a perspective for the layout of the model, and specifically how the various components, structures, and regions lie relative to the reactor core region (i.e., the neutron source).

Because the figures are intended only to provide a general overview of the model, they do not include illustrations of the geometry meshing developed for the model. To provide such detail is beyond the scope of this report.



Notes: This drawing is not to scale.  
 Dimensions are given in centimeters (inches).  
 \* In quadrant symmetry, these capsules represent the 30°, 120° and 300° capsules

Figure 3-2  
 Planar view of the Browns Ferry 2 RAMA quadrant model at the core mid-plane elevation



Notes: This drawing is not to scale.  
Dimensions are given in centimeters (inches).

Figure 3-3  
Axial view of the Browns Ferry 2 RAMA model

The following subsections provide an overview of the computer models that were developed for the various components, structures, and coolant flow regions of the Browns Ferry 2 reactor.

### 3.2.2.1 The Geometry Model

RAMA uses a generalized three-dimensional geometry modeling system that is based on a combinatorial geometry technique, which is mapped to a Cartesian coordinate system. In this analysis, an axial plane of the reactor model is defined by the (x,y) coordinates of the modeling system, and the axial elevation at which a plane exists is defined along a perpendicular z-axis of the modeling system. Thus, any point in the reactor model can be addressed by specifying the (x,y,z) coordinates for that point.

Figure 3-1 illustrates a planar cross-section view of the Browns Ferry 2 reactor design at an axial elevation corresponding to the reactor core mid-plane elevation. It is shown for this one elevation that the reactor design is a complex geometry composed of various combinations of rectangular, cylindrical, and wedge-shaped bodies. When the reactor is viewed in three dimensions, the varying heights of the different components, structures, and regions create additional geometry modeling complexities. An accurate representation of these geometrical complexities in a predictive computer model is essential for calculating accurate, best-estimate fluence in the reactor pressure vessel, the vessel internals, and the surrounding structures.

Figures 3-2 and 3-3 provide general illustrations of the planar and axial geometry complexities that are represented in the Browns Ferry 2 fluence model. For comparison purposes, the planar view illustrated in Figure 3-2 corresponds to the same core mid-plane elevation illustrated in Figure 3-1. The computer model for Browns Ferry 2 assumes azimuthal quadrant symmetry in the planar dimension.

Figure 3-2 illustrates the quadrant geometry that was modeled in this analysis. In terms of the modeling coordinate system, the “northeast” quadrant of the geometry is represented in the model. The 0° azimuth, which has a “north” designation, corresponds to the 0° azimuth referenced in the plan drawings for the reactor pressure vessel. Degrees are incremented clockwise. Thus, the 90° azimuth is designated as the “east” direction. All other components, structures, and regions have been appropriately mirror reflected or rotated to this quadrant based upon their relationship to the pressure vessel orientation to ensure that the fluence is appropriately calculated relative to the neutron source (i.e., the core region). Although symmetry is a modeling consideration, the results presented in this report for the different components and structures are given at their correct azimuths in the plant.

Figure 3-3 illustrates the axial configuration of the primary components, structures, and regions in the fluence model. For discussion purposes, the same components, structures, and regions shown in the planar view of Figure 3-2 are also illustrated in Figure 3-3. Figure 3-3 shows that the axial height of the fluence model spans from a lower elevation just below the jet pump riser inlet to above the core shroud head flange. This axial height covers all areas of the reactor pressure vessel that are expected to exceed a fluence threshold of  $1.0E+17$  n/cm<sup>2</sup> at 54 EFPY.

As previously noted, Figures 3-2 and 3-3 are not drawn precisely to scale. They are intended only to provide a perspective of how the various components, structures, and regions of the reactor are positioned relative to the reactor core region (i.e., the neutron source) and each other. The following subsections provide details on the modeling of individual components, structures, and regions. Please refer to the figures for visual orientation of the components and regions described in the following subsections.

### 3.2.2.2 The Reactor Core and Core Reflector Models

The reactor core contains the nuclear fuel that is the source of the neutrons that irradiate all components and structures of the reactor. The core is surrounded by a shroud structure that serves to channel the reactor coolant through the core region during reactor operation. The region between the core and the core shroud is the core reflector, and it contains coolant. The reactor core geometry is rectangular in design and is modeled with rectangular elements to preserve its shape in the analysis. The core reflector region interfaces with the rectangular shape of the core region and the curved shape of the core shroud. It is, therefore, modeled using a combination of rectangular and cylindrical elements.

The core region is centered in the reactor pressure vessel and is characterized in the analysis with two fundamental fuel zones: interior fuel assemblies and peripheral fuel assemblies. The peripheral fuel assemblies are the primary contributors to the neutron source in the fluence calculation. Because these assemblies are loaded at the core edge where neutron leakage from the core is greatest, there is a sharp power gradient across these assemblies that requires consideration. To account for the power gradient, the peripheral fuel assemblies are sub-meshed with additional rectangular elements that preserve the pin-wise details of the fuel assembly geometry and power distribution. The interior fuel assemblies make a lesser contribution to the reactor fluence and are, therefore, modeled in various homogenized forms in accordance with their contributions to the reactor fluence. For computational efficiency, homogenization treatments are used in the interior core region primarily to reduce the number of mesh regions that must be solved in the transport calculation. The meshing configuration for each fuel assembly location in the core region is determined by parametric studies to ensure an accurate estimate of fluence throughout all regions of the reactor system.

Each fuel assembly design, whether loaded in the interior or peripheral locations in the core, is represented with four axial material zones: the lower tie plate/end plug zone, the fuel zone, the fuel upper plenum zone, and the upper tie plate/end plug zone. The structural materials in the top and bottom nozzles for each unique assembly design are represented in the model to address the shielding effects that these materials have on the components above and below the core region. The fuel zone contains the nuclear fuel and structural materials for the fuel assemblies. The materials for each fuel assembly are unique during reactor operation and are incorporated into the model using reactor operating data from core simulator codes. The upper plenum region captures fission gases during reactor operation.

The Browns Ferry 2 reactor core region has a nominal elevation for the bottom of active fuel at 549.43 cm (216.31 in.) and an active fuel height of 381.00 cm (150 in.). Browns Ferry 2 loaded fuel designs with active fuel heights ranging from 146" to 150". The core simulator codes used by Browns Ferry 2 modeled the core as 150" in all situations, so this value was also used in the RAMA model. Since the predominant peripheral fuel designs throughout Browns Ferry 2's history were 150" in height, the effect of this approximation on the component fluence will be negligible.

From an isotopic standpoint, the core is modeled using quadrant symmetry. For the 30° and 120° capsule evaluations, as well as the peak RPV fluence calculations, the NE fuel quadrant was used.

### 3.2.2.3 The Core Shroud Model

The core shroud is a canister-like structure that contains the reactor core and channels the reactor coolant and steam produced by the core into the steam separators. Axially the shroud extends from the lower shroud wall to the top of the shroud head rim in the model. The core shroud is cylindrical in design and is modeled with pipe elements.

### 3.2.2.4 The Downcomer Region Model

The downcomer region lies between the core shroud and the reactor pressure vessel. It is basically cylindrical in design, but with some geometrical complexities created by the presence of jet pumps and surveillance capsules in the region. The majority of the downcomer region is modeled with pipe segments. The areas of the downcomer containing the jet pumps and specimen capsules are modeled with the appropriate geometry elements to represent their design features and to preserve their radial, azimuthal, and axial placement in the downcomer region. These structures are described further in the following subsections.

### 3.2.2.5 The Jet Pump Model

There are ten jet pump assemblies in the downcomer region of Browns Ferry 2, which provide the main recirculation flow for the core. The jet pumps are modeled at azimuths 30, 60, and 90° in the downcomer region. When symmetry is applied to the model, the 30° location represents the jet pump assemblies that are positioned azimuthally at 30, 150, 210, and 330°; the 60° location represents those at 60, 120, 240, and 300°; and the 90° location represents the jet pump assemblies at 90 and 270°. Note that there are no jet pumps present at the 0- and 180° azimuths of the reactor.

The jet pump model includes representations for the riser, mixer, and diffuser pipes; nozzles; rams head; riser inlet pipe; and riser brace yoke, leafs, and pads. The jet pump assembly design is modeled using cylindrical pipe elements for the jet pump riser and mixer pipes. The riser pipe is correctly situated between the centers of the mixer pipes. The riser brace assembly model includes two leaf structures that attach to the yoke and pad elements.

### 3.2.2.6 The Surveillance Capsule Model

Section 3.1 describes the three surveillance capsules installed in the Browns Ferry 2 reactor. The surveillance capsules are installed near the inner surface of the pressure vessel wall. The surveillance capsules are rectangular in design. Because of this shape, the capsules are not easily implemented in the otherwise cylindrical elements of the downcomer region model. With reference to Figure 3-1, it is observed that the capsules are of small dimensions in the planar geometry and they reside a long distance (view factor) from the core region. Based on these factors, the otherwise rectangular shape of the surveillance capsules can be reasonably approximated in the model with arc elements. The surveillance capsule model also includes a representation for the downcomer water that surrounds the capsule on all sides.

The surveillance capsules are correctly modeled behind the jet pump riser pipes at the 30- and 60° azimuths. When symmetry is applied to the model, the 30° location represents the capsule installed at 30°, while the 60° location represents the capsules at 120 and 300°.

The surveillance capsules are modeled at their correct axial position and height relative to the core region. The surveillance capsules cover about nine percent of the total core height.

#### 3.2.2.7 The Reactor Pressure Vessel Model

The reactor pressure vessel and vessel cladding lie outside the downcomer region and each is cylindrical in design. Both are modeled with pipe elements. The cladding-pressure vessel interface is a key location for RPV fluence calculations and is preserved in the model. This interface defines the inside surface (OT) for the pressure vessel base metal where the RPV fluence is calculated. Browns Ferry 2 has cladding only on the inside surface of the pressure vessel wall.

#### 3.2.2.8 The Vessel Insulation Model

The vessel insulation lies in the cavity region outside the pressure vessel wall. The insulation is cylindrical in design and follows the contour of the pressure vessel wall. It is modeled with pipe elements.

#### 3.2.2.9 The Inner and Outer Cavity Models

The cavity region lies between the pressure vessel and biological structures. As previously described, the vessel insulation lies in the cavity region; thus creating two cavity regions. The inner cavity region lies between the vessel and the insulation. The outer cavity region lies between the vessel insulation and biological shield cladding. The boundaries of the cavity regions follow the contours of the pressure vessel, vessel insulation, and biological shield. The cavity regions are essentially cylindrical in design and are modeled with pipe segments.

#### 3.2.2.10 The Biological Shield Model

The biological shield (concrete) defines the outer most region of the fluence model. The biological shield is basically cylindrical in design and is modeled with pipe segments. There is cladding on the inside and outside surface of the biological shield.

#### 3.2.2.11 The Above-Core Component Models

Figure 3-3 includes illustrations of other components and regions that lie above the reactor core region. The predominant above-core components represented in the model include the top guide and core spray spargers.

##### The Top Guide Model

The top guide component lies above the core region. The top guide is appropriately modeled by including representations for the vertical fuel assembly parts and top guide plates. The upper fuel assembly parts that extend into the top guide region are modeled in three axial segments: the fuel rod plenum, fuel rod upper end plugs, and fuel assembly upper tie plate. The fuel assembly parts and top guide plates are modeled with rectangular elements.

## The Core Spray Sparger Model

The core spray spargers include upper and lower sparger pipes and a vertical inlet pipe. The core spray spargers are appropriately represented as torus structures in the model. The sparger pipes reside inside the upper shroud wall above the top guide. The spargers are modeled as pipe-like structures and include a representation of reactor coolant inside the pipes.

### 3.2.2.12 The Below-Core Component Models

Figure 3-3 includes illustrations of other components and regions that lie below the reactor core region. The fuel support piece, core support plate, and core inlet regions appropriately include a representation of the cruciform control rod below the core region. The lower fuel assembly parts include representations for the fuel rod lower end plugs, lower tie plate, and nose piece. The below-core components are modeled with rectangular elements with the exception of the core support plate. The core support plate is modeled using both rectangular and cylindrical elements to provide an appropriate representation of that component.

### 3.2.2.13 Summary of the Geometry Modeling Approach

To summarize the reactor modeling process, there are several key features of the RAMA code system that allow the reactor design to be accurately represented for RPV and capsule fluence evaluations. Following is a summary of some of the key features of the model.

- Rectangular, cylindrical, and wedge bodies are mixed in the model in order to provide an accurate geometrical representation of the components and regions in the reactor.
- The reactor core geometry is modeled with rectangular bodies to represent its actual shape in the reactor. The fuel assemblies in the core region are also sub-meshed with additional rectangular bodies to represent the pin cell regions in the assemblies.
- A combination of rectangular and cylindrical bodies is used to describe the transition parts between the rectangular core region and the cylindrical outer core regions.
- Cylindrical and wedge bodies are used to model the components and regions that extend outward from the core region (core shroud, downcomer, RPV, etc.).
- The surveillance capsules are modeled at their correct radial, azimuthal, and elevational positions behind the jet pumps in the downcomer region.
- The above-core region includes accurate representations of the top guide and core spray spargers.
- The below-core region includes appropriate representations for the fuel support piece, core support plate, core inlet regions, cruciform control rods, and control rod drives.
- The biological shield is appropriately represented as a cylindrical body.

### 3.2.3 RAMA Calculation Parameters

The RAMA transport code uses a three-dimensional deterministic transport method to calculate the neutron flux. The accuracy of the transport method is based on a numerical integration technique that uses ray-tracing to characterize the geometry, anisotropy treatments to determine

the directional flow of particles, and convergence parameters to determine the overall accuracy of the flux solution between iterates. The code allows the user to specify values for each of these parameters.

The primary input parameters that control the ray-tracing calculation are the distance between parallel rays in the planar and axial dimensions, the depth that a particle is tracked when a reflective boundary is encountered, and the number of equally spaced angles in polar coordinates for tracking the particles. Plant-specific values are determined for each of the parameters. The RAMA transport calculation employs a treatment for anisotropy that is based on a Legendre expansion of the scattering cross sections. By default, the RAMA transport calculation uses the maximum order of expansion that is available for each nuclide in the RAMA nuclear data library. For the actinide and zirconium nuclides, a  $P_5$  expansion of the scattering cross sections is used. For all other nuclides, a  $P_7$  expansion of the scattering cross sections is used.

The overall accuracy of the neutron flux calculation is determined using an iterative technique to converge the flux iterations. The convergence criterion used in the evaluation was determined by parametric study to provide an asymptotic solution for this model.

### **3.2.4 RAMA Neutron Source Calculation**

RAMA calculates a unique neutron source distribution for each transport calculation using the input relative power density factors for the fuel region and data from the RAMA nuclear data library. The source distribution changes with fuel burnup; thus, the source is determined using core-specific three-dimensional burnup distributions at frequent intervals throughout a cycle. For the fluence model, the peripheral fuel assemblies are modeled to preserve the power gradient at the core edge that is formed from the pin-wise source distributions in these fuel assemblies.

### **3.2.5 RAMA Fission Spectra**

RAMA calculates a weighted fission spectrum for each transport calculation that is based on the relative contributions of  $^{235}\text{U}$ ,  $^{238}\text{U}$ ,  $^{239}\text{Pu}$ ,  $^{240}\text{Pu}$ ,  $^{241}\text{Pu}$ , and  $^{242}\text{Pu}$  isotopes. The fission spectra for these isotopes are derived from the BUGLE-96 nuclear data library.

## **3.3 Surveillance Capsule Activation and Fluence Results**

This section documents the fluence and activation results for the Browns Ferry 2 reactor. The activation results also form the basis for the validation and qualification of the application of the RAMA Fluence Methodology to the Browns Ferry 2 reactor in accordance with the requirements of U. S. NRC Regulatory Guide 1.190 (Reg. Guide 1.190). Reg. Guide 1.190 requires fluence calculational methods to be validated by comparison with measurements from operating reactor dosimetry for the specific plant being analyzed or for reactors of similar design.

Three flux wire activation analyses were performed for the Browns Ferry 2 reactor. Flux wires were removed from the 30° capsule flux wire holder and analyzed at the end of cycle 1 (irradiated for 1.3 EFPY); surveillance capsule flux wires were removed at the end of cycle 7 from the 30° capsule (irradiated for 8.1 EFPY); and surveillance capsule flux wires were removed at the end of cycle 16 from the 120° capsule (irradiated for 22.9 EFPY). Details of the dosimetry specimens and analysis are presented below.

Peak fluence was calculated for each of the two removed capsules and the 30° capsule flux wire holder. Additionally, peak fluence was calculated for the 300° capsule still in the reactor in support of lead factor calculations. Lead factors are determined and reported for all capsules.

### 3.3.1 Comparison of Predicted Activation to Plant-specific Measurements

The comparison of predicted activation for the Browns Ferry 2 cycles 1, 7, and 16 flux wires to measurements is presented in this subsection. Fluence values are also calculated and reported in Section 3.4.2 for each of the capsule flux wires.

#### 3.3.1.1 Cycle 1 30° Flux Wire Holder Activation Analysis

Copper and iron flux wires were irradiated in the Browns Ferry 2 surveillance capsule flux wire holder at the 30° azimuth during the first cycle of operation. The wires were removed after being irradiated for a total of 1.3 EFPY. Activation measurements were performed following irradiation for the following reactions [19]:  $^{63}\text{Cu} (n,\alpha) ^{60}\text{Co}$  and  $^{54}\text{Fe} (n,p) ^{54}\text{Mn}$ . The precise location of the individual wires within the surveillance capsule flux wire holder is not known, therefore, the activation calculations were performed at the center of the holder.

Table 3-4 provides a comparison of the RAMA calculated specific activities and the measured specific activities for the flux wire specimens. The cycle 1 total flux wire average calculated-to-measured (C/M) value is 0.91 with a standard deviation of  $\pm 0.02$ .

**Table 3-4**  
Comparison of specific activities for Browns Ferry 2 Cycle 1 30° flux wire holder wires (C/M)

Flux Wires	Measured (dps/mg)	Calculated (dps/mg)	Calculated vs. Measured	Standard Deviation
Iron				
Fe-1	58.11	54.05	0.93	---
Fe-2	58.80	54.05	0.92	---
Fe-3	57.44	54.05	0.94	---
Average	58.12	54.05	0.93	0.01
Copper				
Cu-1	3.198	2.808	0.88	---
Cu-2	3.130	2.808	0.90	---
Cu-3	3.053	2.808	0.92	---
Average	3.127	2.808	0.90	0.02
<b>Total Flux Wire Average</b>	---	---	<b>0.91</b>	<b>0.02</b>

### 3.3.1.2 Cycle 7 30° Surveillance Capsule Activation Analysis

Copper, iron, and nickel flux wires were irradiated in the Browns Ferry 2 surveillance capsule at the 30° azimuth during the first 7 cycles of operation. The wires were removed after being irradiated for a total of 8.1 EFPY. Activation measurements were performed following irradiation for the following reactions [8]:  $^{63}\text{Cu} (n,\alpha) ^{60}\text{Co}$ ,  $^{54}\text{Fe} (n,p) ^{54}\text{Mn}$ , and  $^{58}\text{Ni} (n,p) ^{58}\text{Co}$ .

Table 3-5 provides a comparison of the RAMA calculated specific activities and the measured specific activities for the surveillance capsule flux wire specimens. The cycle 7 capsule total flux wire average C/M value is 1.20 with a standard deviation of  $\pm 0.06$ . It is noted that the EOC 7 capsule comparison shows significantly more conservatism than the two other dosimetry evaluations at EOC 1 and EOC 16. It was noted in the original capsule evaluation [8] that the evaluators also showed a similar overestimate that could imply that some other circumstance exists outside both predictive models that caused the capsule to experience less activation than predicted, such as a dislocation of the capsule container. A 20% change in activity can be caused by as little as a 1/4" variation in radial positioning of the capsule.

**Table 3-5**  
Comparison of specific activities for Browns Ferry 2 cycle 7 30° surveillance capsule flux wires (C/M)

Flux Wires	Measured (dps/g)	Calculated (dps/g)	Calculated vs. Measured	Standard Deviation
Iron				
Average <sup>1</sup>	6.05E+04	7.74E+04	1.28	---
Copper				
Average <sup>1</sup>	5.62E+03	6.49E+03	1.15	---
Nickel				
Average <sup>1</sup>	1.07E+06	1.26E+06	1.18	---
Total Flux Wire Average	---	---	1.20	0.06

<sup>1</sup> The source document for the flux wire measurements only provided an average activity that represents the average of three wires for each wire type.

### 3.3.1.3 Cycle 16 120° Surveillance Capsule Activation Analysis

Copper, iron, and nickel flux wires were irradiated in the Browns Ferry 2 surveillance capsule at the 120° azimuth during the first 16 cycles of operation. The wires were removed after being irradiated for a total of 22.9 EFPY. Activation measurements were performed following irradiation for the following reactions:  $^{63}\text{Cu} (n,\alpha) ^{60}\text{Co}$ ,  $^{54}\text{Fe} (n,p) ^{54}\text{Mn}$ , and  $^{58}\text{Ni} (n,p) ^{58}\text{Co}$ .

Table 3-6 provides a comparison of the RAMA calculated specific activities and the measured specific activities for the surveillance capsule flux wire specimens. The cycle 16 capsule total flux wire average C/M value is 1.08 with a standard deviation of  $\pm 0.07$ .

**Table 3-6**  
**Comparison of specific activities for Browns Ferry 2 cycle 16 120° surveillance capsule flux wires (C/M)**

Flux Wires	Measured (dps/mg)	Calculated (dps/mg)	Calculated vs. Measured	Standard Deviation
Iron				
Fe-G9	80.04	91.95	1.15	---
Fe-G10	85.15	91.95	1.08	---
Average	82.60	91.95	1.11	0.05
Copper				
Cu-G9	13.71	13.70	1.00	---
Cu-G10	13.74	13.70	1.00	---
Average	13.73	13.70	1.00	0.00
Nickel				
Ni-G9	1076.30	1226.63	1.14	---
Ni-G10	1120.09	1226.63	1.10	---
	1098.20	1226.63	1.12	0.03
<b>Total Flux Wire Average</b>	---	---	<b>1.08</b>	<b>0.07</b>

### 3.3.1.4 Surveillance Capsule Activation Analysis Summary

Table 3-7 presents a summary of the total average calculated-to-measured result of specific activities for all Browns Ferry 2 flux wires. Combining all flux wires (copper, iron, and nickel), the total average C/M is 1.08 with a standard deviation of  $\pm 0.13$ .

**Table 3-7**  
**Comparison of activities for Browns Ferry 2 surveillance capsule flux wires**

Dosimeter	Number of Measurements	Calculated vs. Measured	Standard Deviation
30° Flux Wire (EOC 1)	6	0.91	0.02
30° Capsule (EOC 7)	9	1.20	0.06
120° Capsule (EOC 16)	6	1.08	0.07
<b>Total</b>	<b>21</b>	<b>1.08</b>	<b>0.13</b>

### 3.3.2 Capsule Peak Fluence Calculations and Lead Factor Determinations

Peak fast neutron ( $E > 1.0$  MeV) fluences were calculated for each of the capsules originally installed in the Browns Ferry 2 reactor. Of the three original capsules, two have been removed, those being the 30- and 120-degree capsules. The third capsule, located at 300°, remains in the reactor. The peak fluences for the 30-degree capsule are reported at the time of their respective removal, while the 120-degree capsule has fluence reported at the end of cycle 16, and at the end of the reactor's extended operating life of 54 EFPY. Additionally, the lead factor for each capsule is calculated by dividing the peak capsule fluence by the respective peak RPV fluence at a given reporting time. The results of these calculations are presented in Table 3-8. Note that since the 300° capsule has not yet been removed, the lead factor and fluence are estimated.

It is observed in Table 3-8 that the lead factors vary between cycles and capsules. In theory, a plant running with a consistent fuel loading pattern and a symmetric power shape will have similar lead factors for all capsules, since the capsules usually reside in symmetric locations. In the case of Browns Ferry 2, the decreased lead factor between the EOC 7 30° capsule and the EOC 16 120° capsule can be attributed to changing fuel designs, as seen in Table 3-2. Like other fluence predictions, any future changes in any of the items listed in "Limitations of Fluence Projections" will impact the 300° capsule lead factor predictions.

**Table 3-8**  
Lead factors for Browns Ferry 2 30°, 120°, and 300° surveillance capsules

Capsule	Time of Removal	EFPY at Removal	Capsule Fluence (n/cm <sup>2</sup> )	RPV Peak Fluence (n/cm <sup>2</sup> )	Lead Factor
30°	EOC 7	8.1 EFPY	2.40E+17	2.29E+17	1.05
120°	EOC 16	22.9 EFPY	6.44E+17	6.30E+17	1.02
300°	EOXL <sup>1</sup> (est.)	54 EFPY	1.60E+18	1.58E+18	1.01

<sup>1</sup>EOXL represents the end of the extended design life, which is assumed to represent 54 EFPY.

### 3.4 Capsule Fluence Uncertainty Analysis

This section presents the combined uncertainty analysis and bias determination for the Browns Ferry 2 capsule fluence evaluation. The combined uncertainty is comprised of the comparison uncertainty factors and an analytic uncertainty factor developed in this section. When combined, these components provide a basis for determining the overall uncertainty ( $1\sigma$ ) and bias in the capsule fluence for this analysis.

The requirements for determining the combined uncertainty and bias for light water reactor fluence evaluations are provided in Regulatory Guide 1.190. The method implemented for determining the combined uncertainty and bias for reactor component fluence is described in the RAMA Theory Manual [17]. Regarding the determination of a bias in the fluence, Regulatory Guide 1.190 provides that an adjustment to the calculated fluence for bias effects is needed if a statistically significant bias exists in the fluence computation.

The results presented in this section show that the combined uncertainty for the Browns Ferry 2 capsule fluence evaluation is 12.2% and that no adjustment for bias effects is required to the calculated capsule fluence reported in Section 3.3 of this report.

The following subsections describe the comparison uncertainties determined in Section 3.3, the determination of the analytic uncertainty, and the determination of the overall combined uncertainty and bias for the Browns Ferry 2 capsule fluence evaluation.

### **3.4.1 Comparison Uncertainty**

Comparison uncertainty factors are determined by comparing calculated activities with activity measurements. For capsule fluence evaluations, two comparison uncertainty factors are considered: an operating reactor comparison uncertainty factor and a benchmark comparison uncertainty factor. The determination of a comparison uncertainty factor based on measurements involves the combination of two measurement components. One component is the variation in the comparison of the calculated-to-measured (C/M) activity ratio and the other accounts for the uncertainty introduced by the measurement process.

#### **3.4.1.1 Operating Reactor Comparison Uncertainty**

The operating reactor, or plant-specific, comparison uncertainty for the Browns Ferry 2 reactor is determined by combining the standard deviation for the activity comparisons with the measurement uncertainty for the plant-specific activity measurements.

#### **3.4.1.2 Benchmark Comparison Uncertainty**

The benchmark comparison uncertainty used in the Browns Ferry 2 uncertainty analysis is based on a set of industry standard simulation benchmark comparisons.

### **3.4.2 Analytic Uncertainty**

The calculational models used for fluence analyses are comprised of numerous analytical parameters that have associated uncertainties in their values. The uncertainty in these parameters needs to be tested for its contribution to the overall fluence uncertainty.

The uncertainty values for the geometry parameters are based upon uncertainties in the dimensional data used to construct the plant geometry model. The uncertainty values for the material parameters are based upon uncertainties in the material densities for the water and nuclear fuel materials and the compositional makeup of typical steel materials.

The uncertainty values for the fission source parameters are based upon uncertainties in the fuel exposure and power factors for the fuel assemblies loaded on the core periphery. The transport method used in the fluence analysis employs a fission source calculation that accounts for the relative contributions of the uranium and plutonium fissile isotopes in the fuel and the relative power density of the fuel in the reactor. Both fission source parameters are derived directly from information calculated by three-dimensional core simulator codes. The uncertainty values for the nuclear cross-section parameters are based upon uncertainties in the number densities for the predominant nuclides that make up the reactor materials.

The uncertainty parameters for the fluence model inputs are based upon geometry meshing and numerical integration parameters used in the neutron flux transport calculation. The process for determining the geometry meshing and numerical integration parameters involves an exhaustive sensitivity study that is described in the RAMA Procedures Manual [18].

### 3.4.3 Combined Uncertainty

The combined uncertainty for the capsule fluence evaluation is determined with a weighting function that combines the analytic, plant-specific comparison, and benchmark comparison uncertainty factors developed in Sections 3.4.1 and 3.4.2. Table 3-9 shows that the combined uncertainty ( $1\sigma$ ) determined for the Browns Ferry capsule fluence is 12.2% for energy >1.0 MeV.

Table 3-9 also shows that, in accordance with Regulatory Guide 1.190, no bias term exists and it is not necessary to adjust the RAMA predicted capsule fluence in this analysis for bias effects. It is also demonstrated in Table 3-9 that the combined uncertainty is within the limits prescribed in U.S. NRC Regulatory Guide 1.190 (i.e.  $\leq 20\%$ ).

**Table 3-9**  
**Combined capsule fluence uncertainty for energy >1.0 MeV**

Uncertainty Term	Value
Combined Uncertainty ( $1\sigma$ )	12.2%
Bias	None <sup>1</sup>

<sup>1</sup> The bias terms are less than their constituent uncertainty values, concluding that no statistically significant bias exists.

# 4

## CHARPY TEST DATA

---

### 4.1 Charpy Test Procedure

Charpy impact tests were conducted in accordance with American Society for Testing and Materials (ASTM) Standards E185-82 and E23-02. The 1982 version of E185 has been reviewed and approved by NRC for surveillance capsule testing applications. This standard references ASTM E23. The tests were conducted using a Tinius Olsen Testing Machine Company, Inc. Model 84 impact test machine with a 300 ft-lb (406.75 J) energy capacity. The Model 84 is equipped with a dial gage as well as the MPM optical encoder system for accurate absorbed energy measurement. The machine is also equipped with an instrumented striker, so a total of three independent measurements of the absorbed energy were made for every test. In all cases, the optical encoder measured energy was reported as the impact energy. The optical encoder energy is much more accurate than the analog dial. The optical encoder can resolve the energy to within 0.04 ft-lbs (0.054 J), whereas, for the dial, the resolution is approximately 0.25 ft-lbs (0.34 J). The impact energy was corrected for windage and friction for each test performed. The velocity of the striker at impact was nominally 18 ft/s (5.49 m/s). The MPM encoder system measures the exact impact velocity for every test. Calibration of the machine was verified as specified in ASTM E23, and verification specimens were obtained from the National Institute for Standards and Technology (NIST) and tested in accordance with the standard.

The ASTM E23 procedure for specimen temperature control using an in-situ heating and cooling system was followed. The advantage of using the MPM in-situ heating/cooling technology is that each specimen is thermally conditioned right up to the instant of impact. Thermal losses associated with liquid bath systems, such as those resulting from transfer from a liquid bath to the test machine, are completely eliminated. Each specimen was held at the desired test temperature for at least 5 minutes prior to testing, and the fracture process zone temperature was held to within  $\pm 1.8^\circ\text{F}$  ( $\pm 1^\circ\text{C}$ ) up to the instant of strike. Precision calibrated tongs were used for specimen centering on the test machine.

Lateral expansion (LE) was determined from measurements made with a lateral expansion gage. The lateral expansion gage was calibrated using precision gage blocks which are traceable to NIST. The percentage of shear fracture area was determined by integrating the ductile and brittle fracture areas using the MPM Digital Optical Comparator (DOC) image analysis system. As shown in Figure 4-1, each fracture surface image is captured, outlined to delineate the brittle area, and outlined to define the outer ductile fracture region. The DOC software then performs a pixel area integration and automatically calculates the shear fracture area. This method for shear area determination is the most accurate method given in ASTM E23 and is far superior to the commonly used photograph comparison method.

The number of Charpy specimens for measurement of the transition region and upper shelf was limited. Therefore, the choice of test temperatures was very important. Prior to testing, the

Charpy energy-temperature curve was predicted using embrittlement models and previous data. The first test was then conducted near the middle of the transition region, and test temperature decisions were then made based on the test results. Overall, the goal was to perform two tests on the upper shelf, and to use the remaining specimens to characterize the 30 ft-lb (41 J) index. This approach was successful and the transition region and upper shelf energy are well defined.

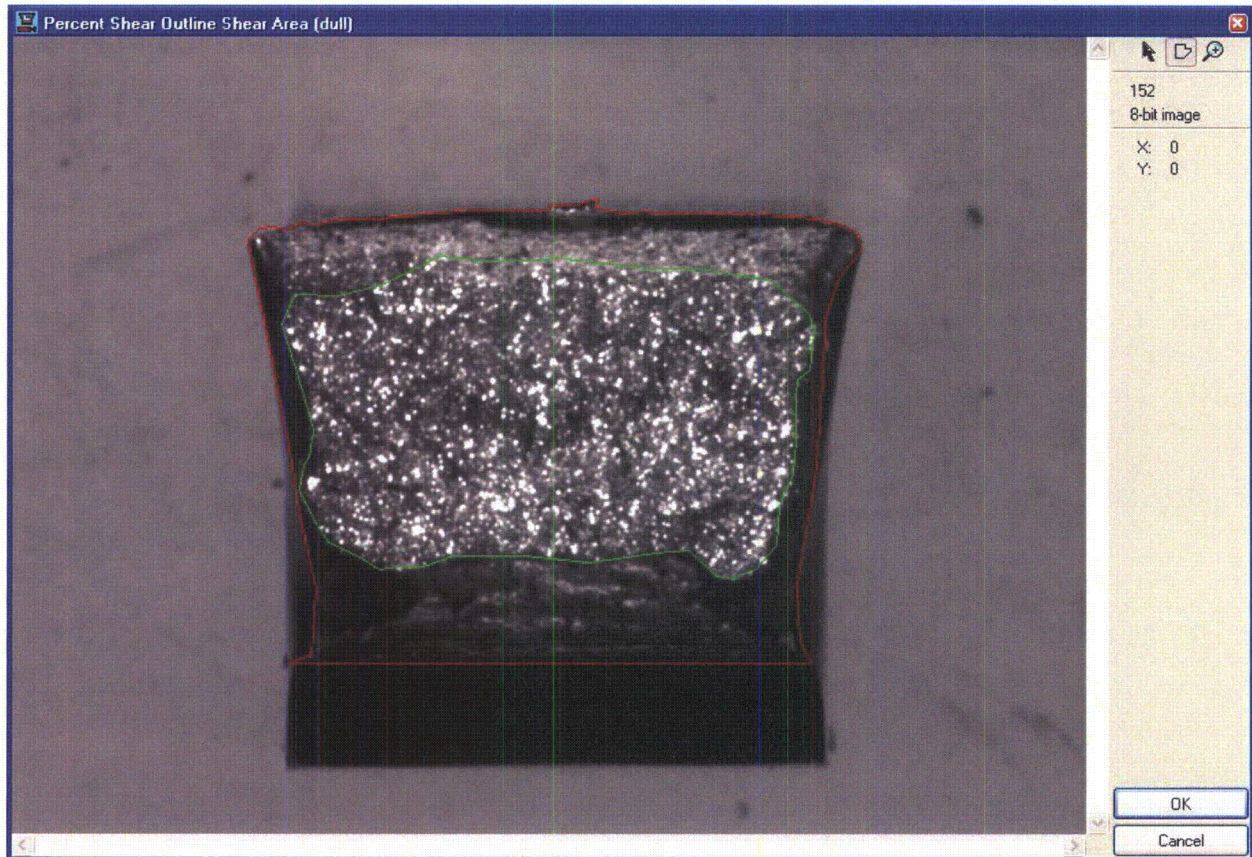


**Figure 4-1**  
**Illustration of digital optical comparator measurement of shear fracture area**

First, the Brittle Fracture Area is outlined (within green line). Next, the Outer Ductile Fracture Area is outlined (within red line). Finally, the software integrates the areas and calculates the Percent Shear Fracture Area.

## 4.2 Charpy Test Data

A total of eight irradiated base, weld, and HAZ metal specimens, respectively, were tested over the transition region temperature range and on the upper shelf. The data are summarized in Tables 4-1 through 4-3. In addition to the energy absorbed by the specimen during impact, the measured lateral expansion values and the percentage shear fracture area for each test specimen are provided in the tables. The Charpy energy was acquired from the optical encoder and has been corrected for windage and friction in accordance with ASTM E23. The impact energy is the energy required to initiate and propagate a crack in the Charpy specimen. The optical encoder and the dial cannot correct for tossing energy or losses in the test machine, and therefore this small amount of additional energy, if present, may be included in the data for some tests. The instrumented striker energy does not include tossing energy or machine vibration energy since

the energy, in this case, is measured only during a few milliseconds of contact between the striker and specimen. Based on comparison between the instrumented striker energy and the optical encoder energy, it has been shown that the tossing energy, and other losses, are small for most tests.

The lateral expansion is a measure of the transverse plastic deformation produced by the contact edge of the striker during the impact event. Lateral expansion is determined by measuring the maximum change of specimen thickness along the sides of the specimen. Lateral expansion is a measure of the ductility of the specimen. The nuclear industry tracks the embrittlement shift using the 35 mil (0.89 mm) lateral expansion index. In accordance with ASTM E23, the lateral expansion for some specimens, which could be broken after the impact test, should not be reported as broken since the lateral expansion of the unbroken specimen is less than that for the broken specimen. Therefore, when these conditions exist, the value listed is the unbroken measurement and a footnote is included to identify these specimens. All of the 120° capsule specimens that did not separate during the test could be broken by hand under the ASTM E23 requirements.

The percentage of shear fracture area is a direct quantification of the transition in the fracture modes as the temperature increases. All metals with a body centered cubic lattice structure, such as ferritic pressure vessel materials, undergo a transition in fracture modes. At low test temperatures, a crack propagates in a brittle manner and cleaves across the grains. As the temperature increases, the percentage of shear (or ductile) fracture increases. This temperature range is referred to as the transition region and the fracture process is mixed mode. As the temperature increases further, the fracture process is eventually completely ductile (i.e., no brittle component) and this temperature range is referred to as the upper shelf region.

**Table 4-1**  
Irradiated Charpy V-Notch impact test results for base metal (heat A0981-1) specimens from the Browns Ferry 2 120° surveillance capsule

Specimen Identification <sup>1</sup>	Test Temperature		Impact Energy		Lateral Expansion		Fracture appearance
	°F	(°C)	ft-lb	(J)	mils	(mm)	% Shear
E7B	-105.3	(-76.3)	4.33	(5.87)	5.0	(0.13)	3.7
E7J	-39.5	(-39.7)	21.92	(29.72)	15.0	(0.38)	11.7
E7C	6.3	(-14.3)	23.08	(31.29)	20.5	(0.52)	20.8
E63	40.1	(4.5)	73.68	(99.90)	54.0	(1.37)	38.2
E75	64.0	(17.8)	99.02	(134.25)	72.5	(1.84)	58.8
E74	97.2	(36.2)	107.05	(145.14)	70.5	(1.79)	60.3
E62	174.7	(79.3)	140.88	(191.01)	92.0	(2.34)	100.0
E5K	327.9	(164.4)	144.72	(196.21)	93.5	(2.37)	100.0

<sup>1</sup> All specimen IDs have a dot over the middle alphanumeric character.

**Table 4-2**  
Irradiated Charpy V-Notch impact test results for weld metal (heat BF2 ESW) specimens from the Browns Ferry 2 120° surveillance capsule

Specimen Identification <sup>1</sup>	Test Temperature		Impact Energy		Lateral Expansion		Fracture appearance
	°F	(°C)	ft-lb	(J)	mils	(mm)	% Shear
EBJ	-49.7	(-45.4)	5.47	(7.42)	6.5	(0.17)	4.6
EAL	14.4	(-9.8)	28.06	(38.04)	21.5	(0.55)	12.7
EAE	50.0	(10.0)	47.89	(64.93)	40.0	(1.02)	22.5
EC3	81.3	(27.4)	22.40	(30.37)	25.0	(0.64)	28.3
EBU	119.1	(48.4)	83.90	(113.75)	63.5	(1.61)	50.3
EB6	204.3	(95.7)	102.15	(138.49)	79.0	(2.01)	79.3
EAK	301.6	(149.8)	113.53	(153.92)	88.0	(2.24)	100.0
EAD	373.8	(189.9)	110.62	(149.98)	84.5	(2.15)	100.0

<sup>1</sup>All specimen IDs have a dot over the middle alphanumeric character.

**Table 4-3**  
Irradiated Charpy V-Notch impact test results for HAZ specimens from the Browns Ferry 2 120° surveillance capsule

Specimen Identification <sup>1</sup>	Test Temperature		Impact Energy		Lateral Expansion		Fracture appearance
	°F	(°C)	ft-lb	(J)	mils	(mm)	% Shear
ED3	-109.5	(-78.6)	2.17	(2.94)	0.5	(0.01)	5.1
EDK	-70.6	(-57.0)	22.95	(31.12)	14.0	(0.36)	15.7
EEL	-12.5	(-24.7)	45.17	(61.24)	35.5	(0.90)	23.6
EE6	23.5	(-4.7)	62.35	(84.53)	48.0	(1.22)	35.8
EEJ	47.3	(8.5)	92.68	(125.66)	70.0	(1.78)	53.0
ED5	72.0	(22.2)	112.58	(152.64)	76.5	(1.94)	80.7
EEA	181.6	(83.1)	122.64	(166.28)	84.5	(2.15)	100.0
EET	300.9	(149.4)	141.24	(191.49)	91.5	(2.32)	100.0

<sup>1</sup>All specimen IDs have a dot over the middle alphanumeric character.

Note: HAZ test results are not used in the BWRVIP ISP.

# 5

## CHARPY TEST RESULTS

---

### 5.1 Analysis of Impact Test Results

For analysis of the Charpy test data, the BWRVIP ISP has selected the hyperbolic tangent (tanh) function as the statistical curve-fit tool to model the transition temperature toughness data. A hyperbolic tangent curve-fitting program named CVGRAPH [10] was used to fit the Charpy V-notch energy and lateral expansion data. Analysis methodology (e.g., definition of upper fixed shelf and lower shelf) followed the BWRVIP conventions established for analysis of all ISP data [21, 22]. The impact energy curve-fits from CVGRAPH are provided in Figures 5-1 (plate A0981-1) and 5-3 (weld BF2 ESW), and the lateral expansion curve-fits are shown in Figures 5-2 (plate A0981-1) and 5-4 (weld BF2 ESW). Because HAZ results are not used in the BWRVIP ISP, that data was not fit.

For the analysis of Charpy energy test data, lower shelf energy was fixed at 2.5 ft-lbs (3.4 J). Upper shelf energy was fixed at the average of all test energies exhibiting shear greater than or equal to 95%, consistent with ASTM Standard E185-82 [3]. For analysis of the lateral expansion test data, the lower shelf was fixed at 1.0 mils; the fixed upper shelf was defined as the average of the lateral expansion test data points at the same test temperatures used to define the fixed upper shelf energy.

### 5.2 Irradiated Versus Unirradiated CVN Properties

Table 5-1 summarizes the  $T_{30}$  [30 ft-lb (41 J) Transition Temperature],  $T_{35\text{mil}}$  [35 mil (0.89 mm) Lateral Expansion Temperature],  $T_{50}$  [50 ft-lb (68 J) Transition Temperature], and Upper Shelf Energy for the unirradiated and irradiated materials and shows the change (shift) from baseline values. The unirradiated values of  $T_{30}$  and  $T_{50}$  were taken from the CVGRAPH fits provided in Figures 2-3 and 2-4; the unirradiated values of  $T_{35\text{mil}}$  were previously determined in [21, 22]. The irradiated values are from the index temperatures determined in Figures 5-1 through 5-4.

Table 5-2 provides a comparison of the measured shifts to predicted shifts for plate heat A0981-1 and weld heat BF2 ESW. Predicted shift is based on the formula provided in Reg. Guide 1.99 Rev. 2 [6] and shown in Note 2 to the table. The fluence was input as  $6.44 \times 10^{17}$  n/cm<sup>2</sup>, as reported in Section 3 for the 120° capsule. For surveillance plate heat A0981-1, the measured shift is within the value expected (e.g., the measured shift is less than predicted shift + margin); however, the measured shift for weld heat BF2 ESW is about 15% greater than the predicted shift + margin.

Measured percent decrease in USE is presented in Table 5-3 and compared to the percent decrease predicted by Figure 2 of Reg. Guide 1.99, Rev. 2. For both the surveillance plate and weld, the measured percent decrease is less than the predicted percent decrease.

**Irradiated Plate Heat A0981-1 CVE (BF2-120)**

CVGRAPH 5.0.2 Hyperbolic Tangent Curve Printed on 09/23/2012 01:19 PM

Page 1

Coefficients of Curve 1

**A = 72.65 B = 70.15 C = 69.29 T0 = 45.34 D = 0.00E+00**

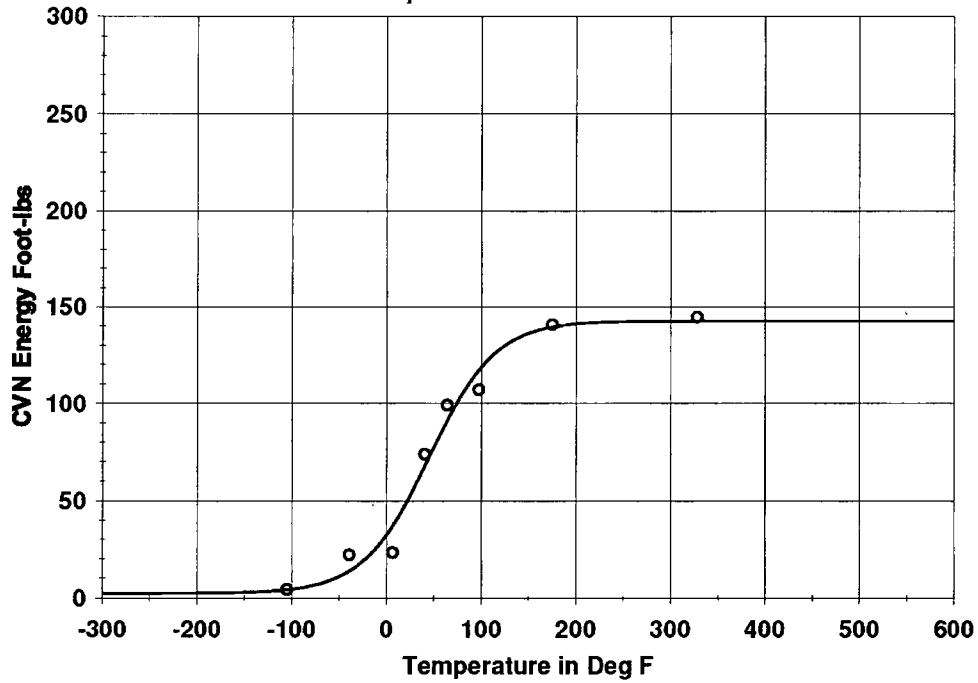
Equation is  $A + B * [\text{Tanh}((T-T_0)/(C+DT))]$

Upper Shelf Energy=142.8(Fixed) Lower Shelf Energy=2.5(Fixed)

Temp@30 ft-lbs=-3.5 Deg F Temp@50 ft-lbs=22.2 Deg F

Plant: BROWNS FERRY 2 Material: SA302BM Heat: A0981-1

Orientation: LT Capsule: 120 DE Fluence: n/cm<sup>2</sup>



**Charpy V-Notch Data**

Temperature	Input CVN	Computed CVN	Differential
- 105.30	4.33	4.29	.04
- 39.50	21.92	13.66	8.26
6.30	23.08	36.84	- 13.76
40.10	73.68	67.36	6.32
64.00	99.02	91.10	7.92
97.20	107.05	117.14	- 10.09
174.70	140.88	139.53	1.35
327.90	144.72	142.76	1.96

Correlation Coefficient = .989

**Figure 5-1  
Irradiated plate A0981-1 (Browns Ferry 2 120° capsule) Charpy energy plot**

**Irradiated Plate Heat A0981-1 LE (BF2-120)**

CVGRAPH 5.0.2 Hyperbolic Tangent Curve Printed on 09/23/2012 01:25 PM  
Page 1

Coefficients of Curve 1

A = 46.88 B = 45.88 C = 69.83 T0 = 34.81 D = 0.00E+00

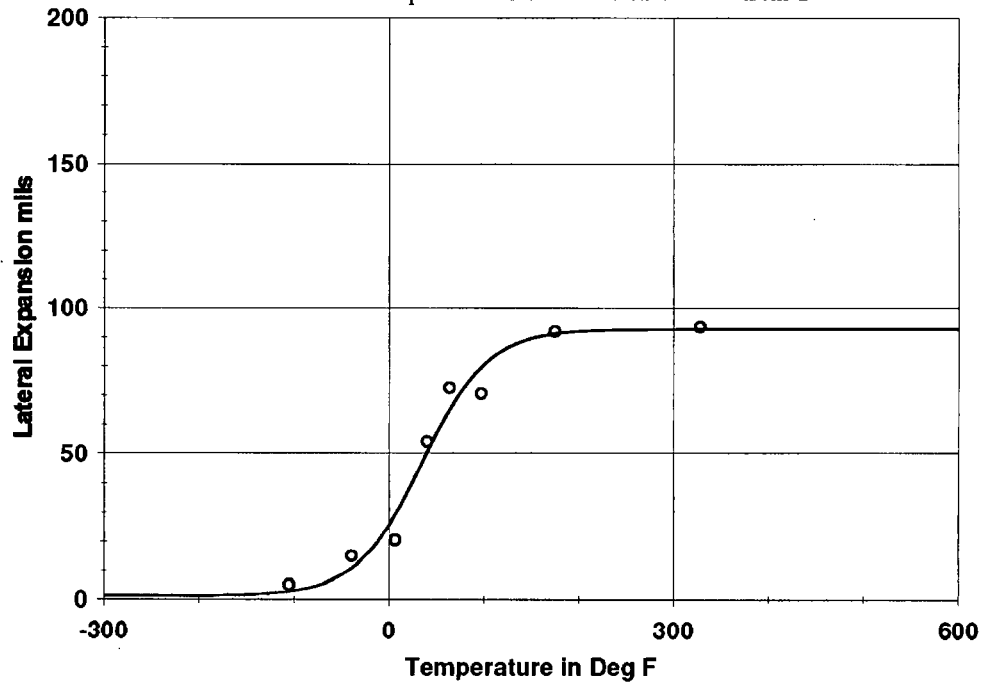
Equation is  $A + B * [\text{Tanh}((T-T_0)/(C+DT))]$

Upper Shelf L.E.=92.8(Fixed) Lower Shelf L.E.=1.0(Fixed)

Temp.@L.E. 35 mils=16.4 Deg F

Plant: BROWNS FERRY 2 Material: SA302BM Heat: A0981-1

Orientation: LT Capsule: 120 DE Fluence: n/cm<sup>2</sup>



**Charpy V-Notch Data**

Temperature	Input L.E.	Computed L.E.	Differential
- 105.30	5.00	2.63	2.37
- 39.50	15.00	10.76	4.24
6.30	20.50	29.12	- 8.62
40.10	54.00	50.34	3.66
64.00	72.50	65.01	7.49
97.20	70.50	79.59	- 9.09
174.70	92.00	91.11	.89
327.90	93.50	92.73	.77

Correlation Coefficient = .986

**Figure 5-2**  
**Irradiated plate A0981-1 (Browns Ferry 2 120° capsule) lateral expansion plot**

**Irradiated Weld Heat BF2 ESW CVE (BF2-120)**

CVGRAPH 5.0.2 Hyperbolic Tangent Curve Printed on 09/23/2012 01:27 PM

Page 1

Coefficients of Curve 1

**A = 57.29 B = 54.79 C = 99.55 T0 = 94.15 D = 0.00E+00**

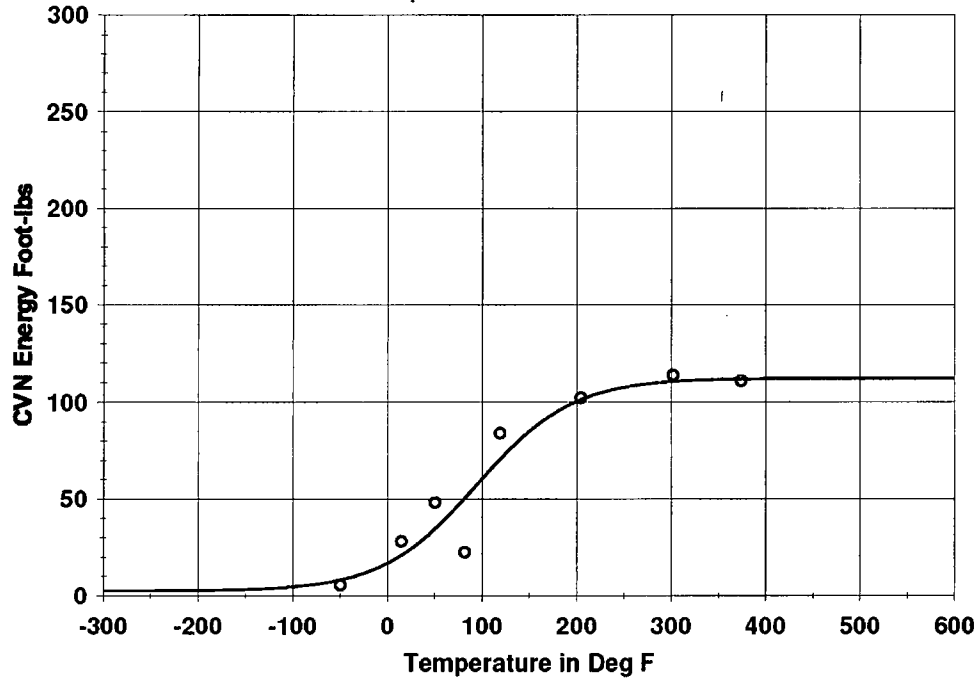
Equation is  $A + B * [\text{Tanh}((T-T_0)/(C+DT))]$

Upper Shelf Energy=112.1(Fixed) Lower Shelf Energy=2.5(Fixed)

Temp@30 ft-lbs=39.8 Deg F Temp@50 ft-lbs=80.9 Deg F

Plant: BROWNS FERRY 2 Material: ESW Heat: ESW

Orientation: NA Capsule: 120 DE Fluence: n/cm<sup>2</sup>



**Charpy V-Notch Data**

Temperature	Input CVN	Computed CVN	Differential
- 49.70	5.47	8.27	- 2.80
14.40	28.06	20.87	7.19
50.00	47.89	34.47	13.42
81.30	22.40	50.26	- 27.86
119.10	83.90	70.74	13.16
204.30	102.15	101.28	.87
301.60	113.53	110.41	3.12
373.80	110.62	111.68	- 1.06

Correlation Coefficient = .954

**Figure 5-3**  
Irradiated weld BF2 ESW (Browns Ferry 2 120° capsule) Charpy energy plot

**Irradiated Weld Heat BF2 ESW LE (BF2-120)**

CVGRAPH 5.0.2 Hyperbolic Tangent Curve Printed on 09/23/2012 01:29 PM

Page 1

Coefficients of Curve 1

A = 43.63 B = 42.63 C = 108.46 T0 = 85.22 D = 0.00E+00

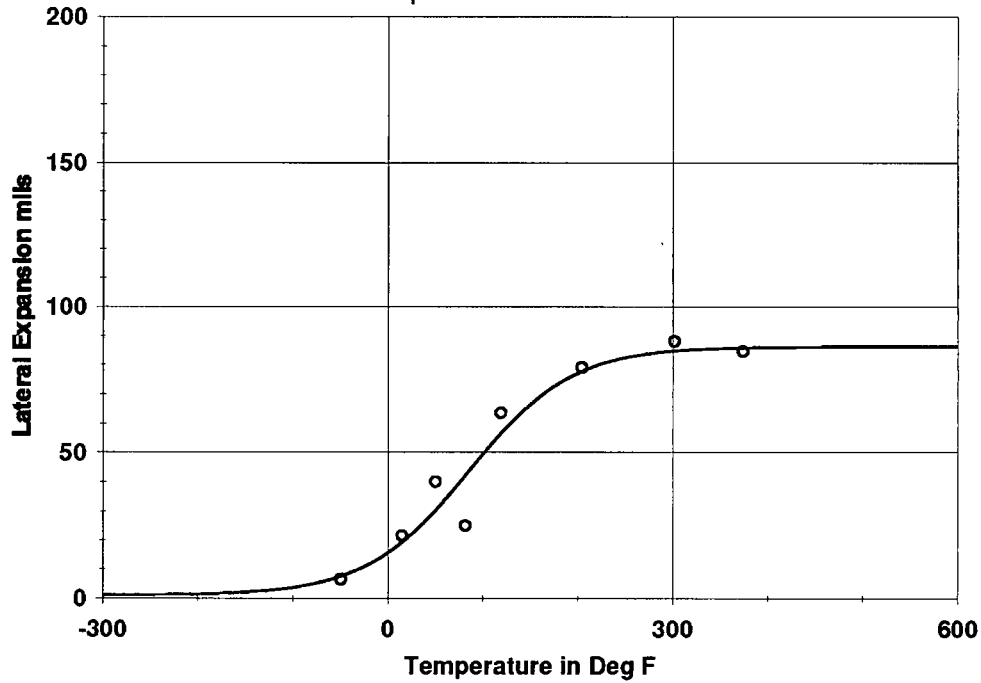
Equation is  $A + B * [\text{Tanh}((T-T_0)/(C+DT))]$

Upper Shelf L.E.=86.3(Fixed) Lower Shelf L.E.=1.0(Fixed)

Temp.@L.E. 35 mils=63.0 Deg F

Plant: BROWNS FERRY 2 Material: ESW Heat: ESW

Orientation: NA Capsule: 120 DE Fluence: n/cm^2



**Charpy V-Notch Data**

Temperature	Input L.E.	Computed L.E.	Differential
-49.70	6.50	7.54	-1.04
14.40	21.50	19.17	2.33
50.00	40.00	30.25	9.75
81.30	25.00	42.09	-17.09
119.10	63.50	56.52	6.98
204.30	79.00	77.71	1.29
301.60	88.00	84.70	3.30
373.80	84.50	85.84	-1.34

Correlation Coefficient = .967

**Figure 5-4**  
Irradiated weld BF2 ESW (Browns Ferry 2 120° capsule) lateral expansion plot

**Table 5-1**  
Effect of irradiation (E>1.0 MeV) on the notch toughness properties

Material Identity	T <sub>30</sub> , 30 ft-lb (41 J) Transition Temperature			T <sub>50</sub> , 50 ft-lb (68 J) Transition Temperature			T <sub>35mil</sub> , 35 mil (0.89 mm) Lateral Expansion Temperature			CVN Upper Shelf Energy (USE)		
	Unirrad °F (°C)	Irradiated °F (°C)	ΔT <sub>30</sub> °F (°C)	Unirrad °F (°C)	Irradiated °F (°C)	ΔT <sub>50</sub> °F (°C)	Unirrad °F (°C)	Irradiated °F (°C)	ΔT <sub>35mil</sub> °F (°C)	Unirrad ft-lb (J)	Irradiated ft-lb (J)	Change ft-lb (J)
A0981-1 (LT)	-46.7 (-43.7)	-3.5 (-19.7)	43.2 (24.0)	-14.8 (-26.0)	22.2 (-5.4)	37.0 (20.6)	-25.4 (-31.9)	16.4 (-8.7)	41.8 (23.2)	137.8 (186.8)	142.8 (193.6)	5.0 (6.8)
BF2 ESW	-52.5 (-46.9)	39.8 (4.3)	92.3 (51.3)	-19.5 (-28.6)	80.9 (27.2)	100.4 (55.8)	-29.5 (-34.2)	63.0 (17.2)	92.5 (51.4)	116.0 (157.3)	112.1 (152.0)	-3.9 (-5.3)

**Table 5-2**  
Comparison of actual versus predicted embrittlement

Identity	Material	Fluence (x10 <sup>17</sup> n/cm <sup>2</sup> )	Measured Shift <sup>1</sup> °F (°C)	RG 1.99 Rev. 2 Predicted Shift <sup>2</sup> °F (°C)	RG 1.99 Rev. 2 Predicted Shift+Margin <sup>2,3</sup> °F (°C)
A0981-1	Browns Ferry 2 Plate (SA533B-1) (LT orientation)	6.44	43.2 (24.0)	32.7 (18.17)	65.43 (36.35)
BF2 ESW	Browns Ferry Unit 2 surveillance weld	6.44	92.3 (51.3)	40.24 (22.36)	80.45 (44.72)

## Notes:

1. See Table 5-1, ΔT<sub>30</sub>.
2. Predicted shift = CF × FF, where CF is a Chemistry Factor taken from tables from USNRC Reg. Guide 1.99, Rev. 2 [6], based on the material's Cu/Ni content, and FF is Fluence Factor,  $f^{0.28-0.10 \log f}$ , where f = fluence (10<sup>19</sup> n/cm<sup>2</sup>, E > 1.0 MeV) specified.
3. Margin Term is defined as 34°F for plate materials and 56°F for weld materials, or margin equals shift (whichever is less), per Reg. Guide 1.99, Rev. 2 [6].

**Table 5-3**  
**Percent decrease in upper shelf energy**

Identity	Material	Fluence ( $\times 10^{17}$ n/cm <sup>2</sup> )	Cu Content (wt%)	Measured Decrease in USE <sup>1</sup> (%)	Predicted Decrease in USE <sup>2</sup> (%)
A0981-1	Browns Ferry 2 Plate A0981-1	6.44	0.14	-3.63	12.0
BF2 ESW	Browns Ferry 2 ESW	6.44	0.20	3.36	17.8

Notes:

1. Calculated from Table 5-1, (Change/Unirradiated) \* 100. A positive number indicates a decrease in USE; a negative number indicates the USE increased over the unirradiated value.
2. Based on extrapolation of and interpolation between the curves given in Figure 2 of Reg. Guide 1.99 Rev. 2 [6].

# 6

## REFERENCES

---

1. 10 CFR 50, Appendices G (*Fracture Toughness Requirements*) and H (*Reactor Vessel Material Surveillance Program Requirements*), Federal Register, Volume 60, No. 243, dated December 19, 1995.
2. American Society of Mechanical Engineers (ASME) Boiler and Pressure Vessel Code (Code), Section XI, "Rules for Inservice Inspection of Nuclear Power Plant Components," Nonmandatory Appendix G, Fracture Toughness Criteria for Protection Against Failure.
3. ASTM E185-82, *Standard Practice for Conducting Surveillance Tests for Light-Water Cooled Nuclear Power Reactor Vessels*, E706 (IF), ASTM Standards, Section 3, American Society for Testing and Materials, Philadelphia, PA, 1993.
4. *BWRVIP-86, Revision 1-A: BWR Vessel and Internals Project, Updated BWR Integrated Surveillance Program (ISP) Implementation Plan*. EPRI, Palo Alto, CA: 2012. 1025144.
5. 10 CFR 50, Appendix B, "Quality Assurance Criteria for Nuclear Power Plants and Fuel Reprocessing Plants."
6. U.S. NRC Regulatory Guide 1.99, "Radiation Embrittlement of Reactor Vessel Materials," Revision 2, May 1988.
7. "Guideline for the Management of Materials Issues," NEI 03-08, Nuclear Energy Institute, Washington, DC, Latest Edition.
8. "Browns Ferry Steam Electric Station Unit 2 Vessel Surveillance Materials Testing and Fracture Toughness Analysis", C. Oza, GE Nuclear Energy, GENE-B1100639-01, Revision 1, August, 1995.
9. Letter from R.H. Shell (TVA) to USNRC, "Browns Ferry Nuclear Plant, Sequoyah Nuclear Plant, and Watts Barr Nuclear Plant – Response to Generic Letter 92-01 (Reactor Vessel Structural Integrity)," Tennessee Valley Authority, dated July 7, 1992.
10. CVGRAPH, Hyperbolic Tangent Curve Fitting Program, Developed by EPRI, Version 5.0.2, Revision 1, 3/26/02.
11. "Calculational and Dosimetry Methods for Determining Pressure Vessel Neutron Fluence," Nuclear Regulatory Commission Regulatory Guide 1.190, March 2001.
12. *BWRVIP-126: BWR Vessel Internals Project, RAMA Fluence Methodology Software, Version 1.0*. EPRI, Palo Alto, CA: 2003. 1007823.
13. Letter from William H. Bateman (U.S. NRC) to Bill Eaton (BWRVIP), Safety Evaluation of Proprietary EPRI Reports BWRVIP-114, -115, -117, and -121 and TWE-PSE-001-R-001. dated May 13, 2005.

---

References

14. Letter from Matthew A. Mitchell (U.S. NRC) to Rick Libra (BWRVIP), "Safety Evaluation of Proprietary EPRI Report BWR Vessel and Internals Project, Evaluation of Susquehanna Unit 2 Top Guide and Core Shroud Material Samples Using RAMA Fluence Methodology (BWRVIP-145)," dated February 7, 2008.
15. "BUGLE-96: Coupled 47 Neutron, 20 Gamma-Ray Group Cross Section Library Derived from ENDF/B-VI for LWR Shielding and Pressure Vessel Dosimetry Applications," RSICC Data Library Collection, DL2C-185, March 1996.
16. "VITAMIN-B6: A Fine-Group Cross Section Library Based on ENDF/B-VI Release 3 for Radiation Transport Applications," RSICC Data Library Collection, DL2C-184, December 1996.
17. *BWRVIP-114-A: BWR Vessel and Internals Project, RAMA Fluence Methodology Theory Manual*, EPRI, Palo Alto, CA: 2009. 1019049.
18. *BWRVIP-121-A: BWR Vessel and Internals Project, RAMA Fluence Methodology Procedures Manual*, EPRI, Palo Alto, CA: 2009. 1019052.
19. Analysis of the Vessel Wall Neutron Dosimeter from Browns Ferry Unit 2 Pressure Vessel, Southwest Research Institute, 02-4884-002, Rev. 0, September 1979.
20. ASTM Standard E23, 2002, "Standard Test Methods for Notch Bar Impact Testing of Metallic Materials," ASTM International, West Conshohocken, PA, 2002, DOI: 10.1520/E0023-02, www.astm.org.
21. *BWRVIP-135, Revision 2: BWR Vessel and Internals Project, Integrated Surveillance Program (ISP) Data Source Book and Plant Evaluations*. EPRI, Palo Alto, CA: 2009. 1020231.
22. BWRVIP Letter 2010-238, Errata for BWRVIP-135, Rev. 2, October 15, 2010.

# A

## APPENDIX A – DOSIMETER ANALYSIS

---

### A.1 Dosimeter Material Description

The 120° Browns Ferry Unit 2 (BF2) surveillance capsule primary dosimeter materials are pure metal wires which were located within the surveillance capsule Charpy packets. The wire types provided for the Browns Ferry Unit 2 surveillance program are copper, iron, and nickel. Each wire is about three inches (7.62 cm) long with one of each type included in the two Charpy specimen packets.

### A.2 Dosimeter Cleaning and Mass Measurement

At the time the Charpy packets were opened, the dosimeter wires were cleaned with wipes that were wetted with acetone to remove loose contamination. Upon receipt at the radiometric lab, the wires were visually inspected and cleaned with a lab wipe soaked in pure ethanol. The wire segments were then examined under a low magnification optical microscope. There was evidence of oxidation indicating the need for chemical etching and further cleaning. This was accomplished by soaking the Fe wire segments in a 4N solution of hydrochloric acid until the oxidation was etched from the surface. Similarly, the Ni and Cu wires were immersed in a 2N solution of nitric acid solution. The wires were then rinsed with distilled water, wiped once more with ethanol, and then allowed to dry in air at room temperature. The wires then exhibited a clean, shiny appearance. Figures A-1 through A-6 show low-power magnifications of the dosimetry wires as they were found prior to cleaning, and after cleaning and coiling. In general, the iron and copper wires had experienced the most oxidation, while the nickel wires were relatively clean at the time of recovery from the Charpy packets.

The total mass of each wire was measured using a Mettler Toledo XS105DU analytical digital balance. Table A-1 lists the results of these measurements, as well as the identification assigned to each dosimeter. The dosimeters identifications were assigned as the Charpy packet numbers followed by the type of dosimeter material.

As previously mentioned, the wires were tightly coiled for subsequent counting and weighing. Each wire was wrapped around a thin metal rod to form a coil of approximately 0.5 inch (12.7 mm) diameter or less, which yields a reasonable approximation to a point source geometry at the distance the dosimeter wires are placed from the gamma detector. The coiled wire segments were pressed firmly against a hard surface to flatten the coil to yield the best counting geometry

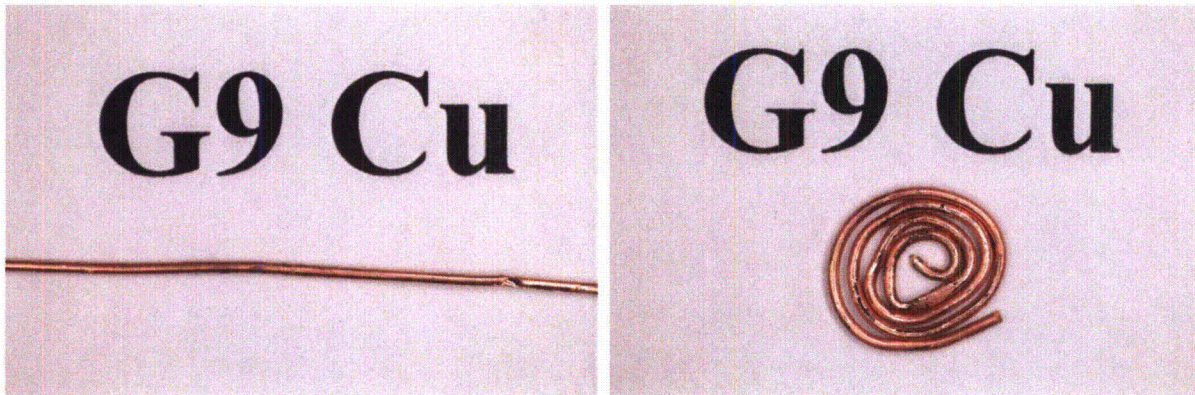


Figure A-1  
Packet G9 Cu dosimeter wire: prior to cleaning (left); and after cleaning/coiling (right)

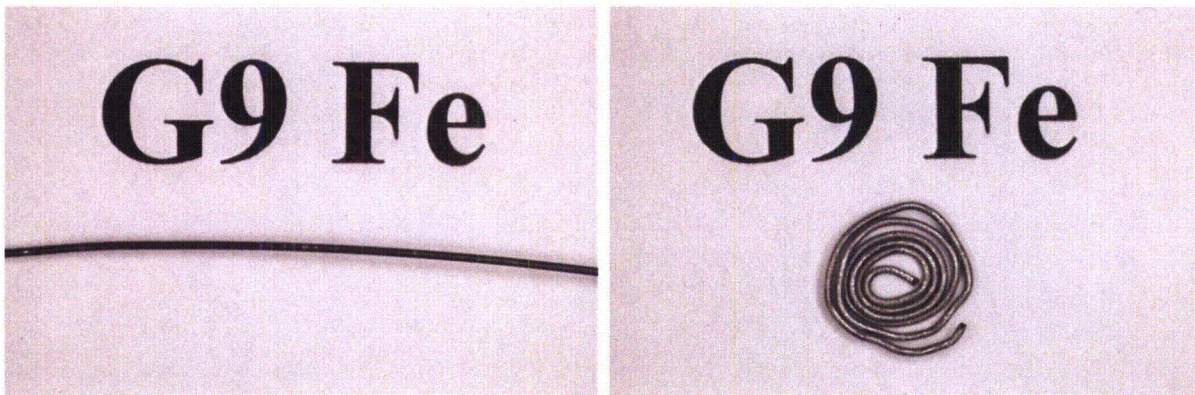


Figure A-2  
Packet G9 Fe dosimeter wire: prior to cleaning (left); and after cleaning/coiling (right)

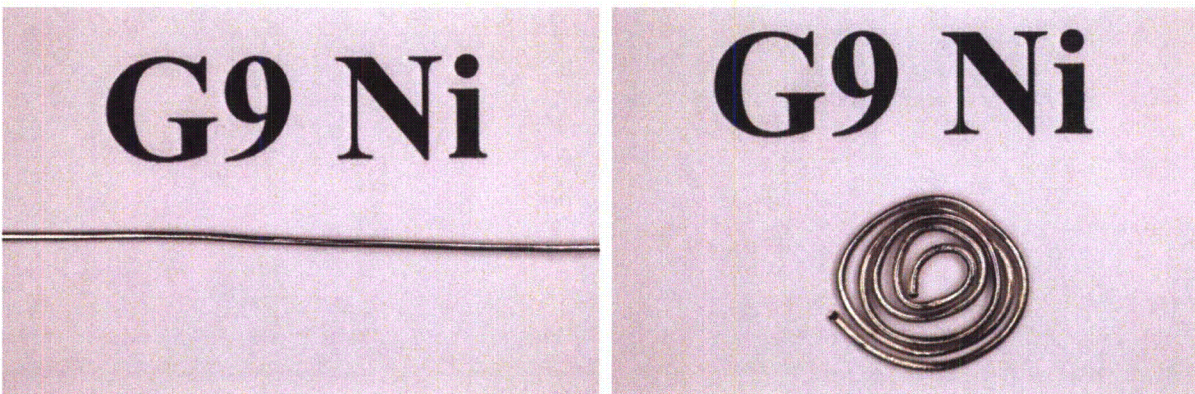


Figure A-3  
Packet G9 Ni dosimeter wire: prior to cleaning (left); and after cleaning/coiling (right)

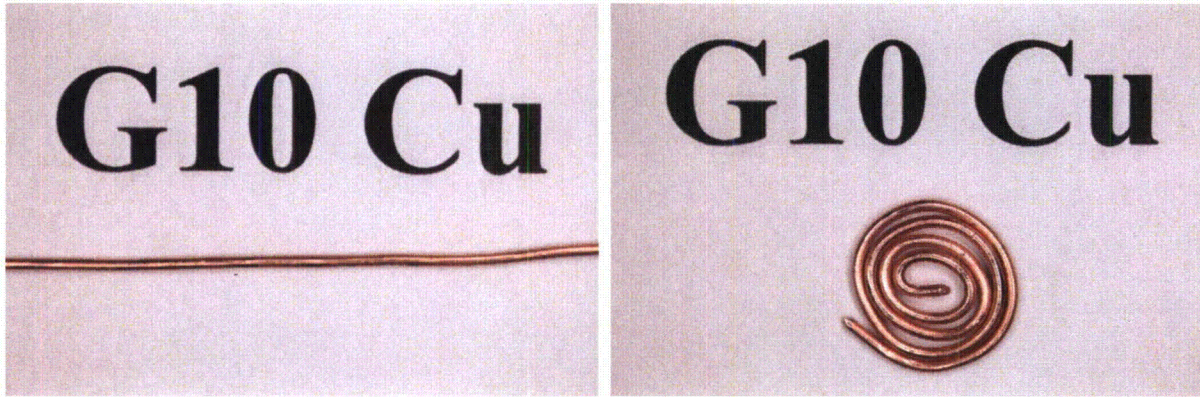


Figure A-4  
Packet G10 Cu dosimeter wire: prior to cleaning (left); and after cleaning/coiling (right)

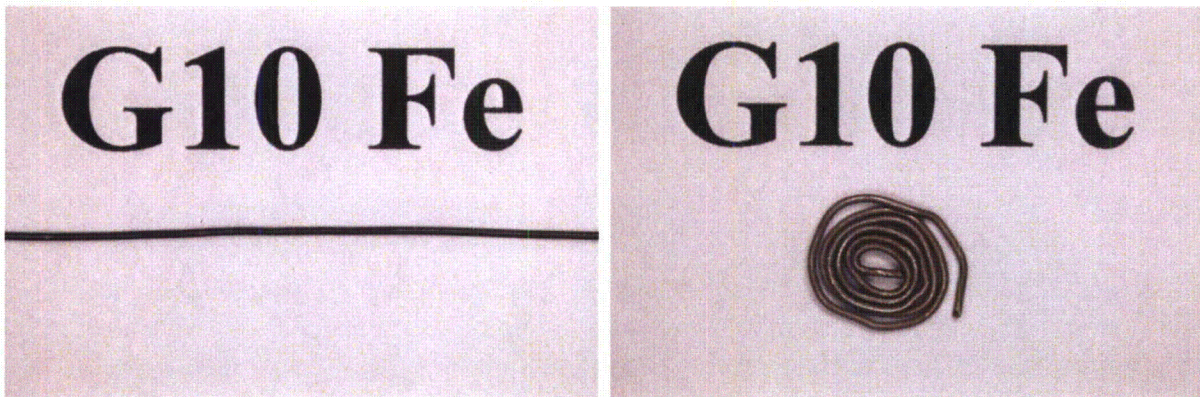


Figure A-5  
Packet G10 Fe dosimeter wire: prior to cleaning (left); and after cleaning/coiling (right)

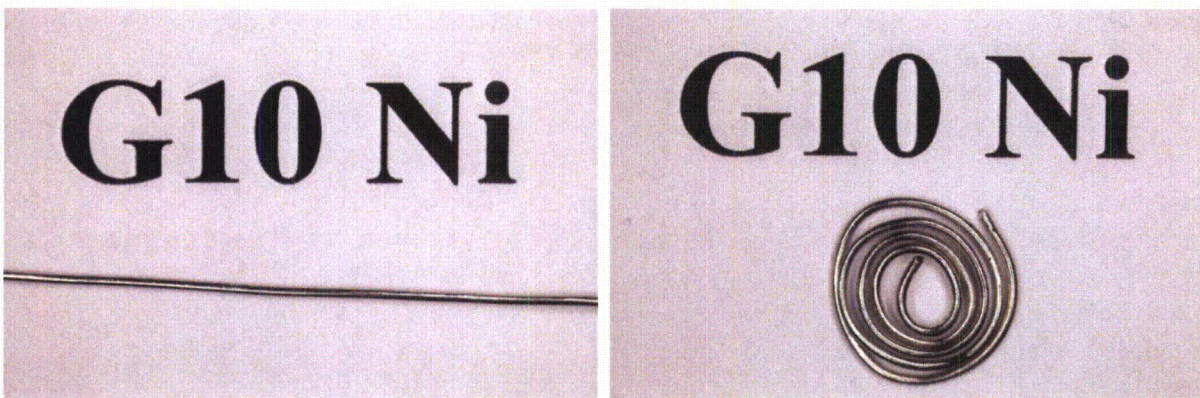


Figure A-6  
Packet G10 Ni dosimeter Wire: prior to cleaning (left); and after cleaning/coiling (right)

**Table A-1**  
**Wire dosimeter masses**

Wire Dosimeter ID	Mass (mg)
G9 Cu	361.65
G9 Fe	159.02
G9 Ni	320.05
G10 Cu	360.86
G10 Fe	160.34
G10 Ni	318.77

### A.3 Radiometric Analysis

Radiometric analysis was performed using high resolution gamma emission spectroscopy. In this method, gamma emissions from the dosimeter materials are detected and quantified using solid-state gamma ray detectors and computer-based signal processing and spectrum analysis. The specifications of the gamma ray spectrometer system (GRSS) are listed in Table A-2. The GRSS features a hyper pure germanium (HPGe) detector that is housed in a lead-copper shield to reduce background count rates. Standard background subtraction procedures were used.

GRSS calibration was performed using a National Institute for Standards and Technology (NIST) traceable mixed gamma quasi-point source. The Canberra analysis software provides the capability for energy resolution and efficiency calibration using specified standard source information. Calibration information is stored on magnetic disk for use by the spectrographic analysis software package.

Since detector efficiency depends on the source-detector geometry, a fixed, reproducible geometry must be selected for the gamma spectrographic analysis of the dosimeter materials. For the dosimeter wires, the counting geometry was that of a quasi-point source (coiled wire) placed five inches (12.7 cm) vertically from the top surface of the detector shell. In this way, extended sources up to 0.5 inch (1.27 cm) can be analyzed with a good approximation to a point source. The coiled wires were well within the area needed to approximate a point source geometry. The HPGe detector was calibrated for efficiency using the NIST traceable source. The accuracy of the efficiency calibration was checked using a gamma spectrographic analysis of the NIST traceable mixed gamma source. The isotopes contained in the source emit gamma rays which span the energy response of the detector for the dosimeter materials. These measurements show that the efficiency calibration is providing a valid measurement of source activity. The acceptance criteria for these measurements are that the software must yield a valid isotopic identification, and that the quantified activity of each correctly identified isotope must be within the uncertainty specified in the source certification. Validation of system performance was performed prior to starting the counting tasks, and upon completion of all counting work for BF2. The counting system performance was acceptable in each case, indicating that the counting system properties did not change during the course of the counting procedure.

Table A-3 shows the counting schedule established for this work. There was no requirement for order of counting, since the dosimeter materials still contained sufficient quantities of activation products to allow accurate radio assay. Counting times were more than sufficient to achieve the desired statistical accuracy for gamma emissions of interest in all cases.

Neutrons interact with the constituent nuclei of the dosimeter materials, producing radionuclides in varying amounts depending on total neutron fluence, its energy spectrum, and the nuclear properties of the dosimeter materials. Table A-4 lists the reactions of interest and their resultant radionuclide products for each element contained in the dosimeters. These are threshold reactions involving an n-p or n- $\alpha$  interaction.

Finally, Table A-5 presents the primary results of interest for flux and fluence determination. The specific activity units are in dps/mg, which normalizes the activity to dosimeter mass. The activities are specified for a useful reference date/time, which in this case is the BF2 plant shutdown date and time. This reference date/time was specified as February 26, 2011, at 12:00:00 AM EST.

**Table A-2**  
**GRSS specifications**

<b>System Component</b>	<b>Description and/or Specifications</b>
Detector	Canberra Model GC1518
Energy Resolution	1.8keV @ 1.33 MeV
Detector Efficiency (relative to a 3 inch x 3 inch (7.62 cm x 7.62 cm) NaI crystal)	15% at 1.3 MeV
Amplifier/Multichannel Analyzer	Canberra DAS-1000
Computer System	Intel i5-2500 CPU at 3.30 GHz., 2.91 GB Main Memory, 931 GB Hard Disk, 17-inch Monitor, HP LaserJet Printer
Software	Canberra Apex v 1.2

**Table A-3**  
Counting schedule for the dosimeter materials

Dosimeter ID	Count Start Date	Count Start Time (ET)	Count Duration (Live Time Seconds)
G9 Cu	08/18/12	2:04 PM	86,400
G9 Fe	08/17/12	1:34 PM	86,400
G9 Ni	08/20/12	6:51 AM	86,400
G10 Cu	08/22/12	8:05 AM	86,400
G10 Fe	08/21/12	7:48 AM	86,400
G10 Ni	08/23/12	8:47 AM	86,400

**Table A-4**  
Neutron-induced reactions of interest

Dosimeter Material	Neutron-Induced Reaction	Reaction Product Radionuclide
Iron	$\text{Fe}^{54}(n,p)\text{Mn}^{54}$	$\text{Mn}^{54}$
Copper	$\text{Cu}^{63}(n,\alpha)\text{Co}^{60}$	$\text{Co}^{60}$
Nickel	$\text{Ni}^{58}(n,p)\text{Co}^{58}$	$\text{Co}^{58}$

**Table A-5**  
Results of the radiometric analysis

Dosimeter ID	Isotope ID	Activity at Reference Date/Time <sup>a</sup> ( $\mu\text{Ci}$ )	Specific Activity at Reference Date/Time <sup>a</sup> (dps/mg)	Activity Uncertainty (%)
G9 Cu	60Co	1.34E-01	13.71	1.90
G9 Fe	54Mn	3.44E-01	80.04	2.56
G9 Ni	58Co	9.31E+00	1076.30	2.74
G10 Cu	60Co	1.34E-01	13.74	1.90
G10 Fe	54Mn	3.69E-01	85.15	2.56
G10 Ni	58Co	9.65E+00	1120.09	2.76

<sup>a</sup> February 26, 2011 at 12:00:00 AM EST is the reference date and time.

**The Electric Power Research Institute, Inc.** (EPRI, [www.epri.com](http://www.epri.com)) conducts research and development relating to the generation, delivery and use of electricity for the benefit of the public. An independent, nonprofit organization, EPRI brings together its scientists and engineers as well as experts from academia and industry to help address challenges in electricity, including reliability, efficiency, affordability, health, safety and the environment. EPRI also provides technology, policy and economic analyses to drive long-range research and development planning, and supports research in emerging technologies. EPRI's members represent approximately 90 percent of the electricity generated and delivered in the United States, and international participation extends to more than 30 countries. EPRI's principal offices and laboratories are located in Palo Alto, Calif.; Charlotte, N.C.; Knoxville, Tenn.; and Lenox, Mass.

Together...Shaping the Future of Electricity

**Programs:**

Nuclear Power

BWR Vessel and Internals Project

© 2013 Electric Power Research Institute (EPRI), Inc. All rights reserved. Electric Power Research Institute, EPRI, and TOGETHER...SHAPING THE FUTURE OF ELECTRICITY are registered service marks of the Electric Power Research Institute, Inc.

3002000078

**Electric Power Research Institute**

3420 Hillview Avenue, Palo Alto, California 94304-1338 • PO Box 10412, Palo Alto, California 94303-0813 USA  
800.313.3774 • 650.855.2121 • [askepri@epri.com](mailto:askepri@epri.com) • [www.epri.com](http://www.epri.com)